JOURNAL OF
The Electrochemical Society

VOLUME 95 NUMBER 4

April 1949

Published Monthly by
THE ELECTROCHEMICAL SOCIETY

Journal of
The Electrochemical Society

Number 4 April 1949 Volume 96

Current Affairs

Editorial
"Give Me Liberty Or—" 73C
Philadelphia Convention Preview 74C
Silicon Carbide Plant Opened 76C
Uhlig Heads Corrosion Committee 77C
Gordon Research Conference on Corrosion 78C
Section News 78C
Personals 82C
New Members 83C
Employment Situations 84C
Recent Patents 84C

Feature Section

The Profession of Electrochemistry
III. Opportunities in the Electroprocess Industries. *R. M. Burns* 85C

Technical Notes and Reviews

Physical Properties of Iron Deposited from Chloride Baths. *I. Larson, R. W. Moulton, and C. L. Putnam* 86C

Technical Papers

Natural Convection in Electrolytic Processes. *Carl Wagner* 161
Basic Sulfates of Lead. *J. J. Lander* 174
Calcium Halophosphate Phosphors. *R. Nogy, R. W. Wollentin, and C. K. Lui* 187
Decay of Phosphorescence and the Mechanism of Luminescence of Zinc Sulfide Phosphors. *W. H. Byler and G. P. Kirkpatrick* 194

EDITORIAL STAFF

H. H. Uhlig
Editor

Eleanor Reid
Managing Editor

H. B. Linford
U. B. Thomas
Associate Editors

R. M. Burns
Consultant

PUBLICATION COMMITTEE

H. J. Read
Chairman

J. M. Bialosky
Paul S. Brallier
N. C. Cahoon
C. L. Faust
H. C. Froelich
A. E. Pavlish
E. B. Saubar
Sherlock Swann, Jr.
Archie J. Weith

Published monthly by The Electrochemical Society, Inc., Mt. Royal and Guilford Aves., Baltimore 2, M... Editorial office: 216 W. 103rd Street, New York 25, N. Y. Statements and opinions given in articles a... papers in the Journal of The Electrochemical Society are those of the contributors and The Electrochemical ... does not assume responsibility for them. Subscription: $7.50 to members and $10 to non-members. Sin... copies $2.50 to members, $3.00 to non-members. Copyright 1949 by The Electrochemical Society, Inc.

Entered as second-class matter November 15, 1947, at the Post Office at Baltimore, Maryland, under the a... of August 24, 1912.

THE ROLE OF NATURAL CONVECTION IN ELECTROLYTIC PROCESSES[1]

CARL WAGNER[2]

Eduard Zintl Institut fuer anorganische und physikalische Chemie der Technischen Hochschule Darmstadt, Germany

ABSTRACT

It is shown both theoretically and experimentally that at a vertical electrode a well-defined convective flow due to the generally smaller density in the boundary layer and the resulting buoyancy force exists, analogous to natural convection in the case of heat transfer from a radiator to ambient air. The interplay between diffusion and convective flow determines the limiting current density which occurs if such a voltage is applied that the concentration of one of the reactants at the electrode drops to zero. Observed values of the limiting current density in a solution of copper sulfate and sulfuric acid are close to calculated values.

INTRODUCTION

When a metal is deposited on a cathode, the concentration of the cations in the solution adjacent to the electrode decreases, for according to Faraday's law 96,500 coulombs reduce one equivalent of cations, but in the solution cations as well as anions participate in the transport of electricity. Because of the deficit of cations at the cathode, cations diffuse toward this electrode. Thus there results a superposition of migration of cations due to the applied electric field and diffusion due to the concentration gradient. The solution being at rest, the current density being given, and the anode being sufficiently remote, H. F. Weber (1), S. R. Milner (2), and others have shown both theoretically and experimentally that the cation concentration at the cathode decreases as a linear function of the square root of time. When the concentration of the cations at the cathode approaches zero, a new cathodic process starts, which in many instances is development of hydrogen. The drop of the cation concentration to zero is to be expected at rather moderate current densities several minutes after the beginning of electrolysis. Actually, much greater current densities than calculated can be applied in the case of vertical electrodes because convection takes place and thus decreases the "diffusion path," which has been calculated from saturation currents by various authors, e.g., R. E. Wilson and M. A. Youtz (3); and S. Glasstone (4). Under the conditions applied, a value of about 0.05 cm. has been found. The nature of such a convective flow has not been expounded in most papers. R. Edgeworth-Johnston (5) has suggested that there is a definite convective flow, similar to natural convection in the case of heat transfer, as a result of the density differences due to the variations of concentrations. This hypothesis is confirmed in the present paper theoretically and experimentally.

[1] Manuscript received August 14, 1948. This paper prepared for delivery before the Philadelphia Meeting, May 4 to 7, 1949.

[2] Present address: Ordnance Research and Development Division Sub-Office (Rocket), Fort Bliss, Texas.

ELECTROCHEMICAL EQUATIONS

Primarily we are interested in the concentration of the cations which are reduced at the cathode. In addition, however, we have to expect an increase of the concentration of other cations such as hydrogen ions, which are driven by the electric field toward the cathode but do not react there, and a decrease of the concentrations of anions driven toward the anode. Referring to the following calculation of the density in the boundary layer, we inquire into the concentrations of all constituents of the solution.

In a solution at rest, the quantity of the ions of type i passing the cross-sectional area A per unit time toward the cathode (in terms of mols per second) equals

$$\frac{dn_i}{dt} = \mathrm{A}\mathrm{D}_i \frac{\partial c_i}{\partial y} + \mathrm{A}c_i \mathrm{U}_i z_i e \frac{\partial \varphi}{\partial y} \tag{1}$$

where y represents the distance from the cathode, D_i the diffusion coefficient, c_i the concentration (in terms of mols per cm.^{3}), φ the electrical potential, z_i the electrical valence (positive for cations, negative for anions), e the electronic charge, and U_i the mobility, here defined as the steady-state velocity when a force equal to unity acts on an individual ion. The diffusion coefficient D_i and the mobility U_i are interrelated by the well-known equation

$$\mathrm{D}_i = \mathrm{U}_i k\mathrm{T} \tag{2}$$

where k is the Boltzmann constant and T the temperature.

Eliminating U_i in equation (1), we obtain

$$\frac{dn_i}{dt} = \mathrm{A}\mathrm{D}_i \frac{\partial c_i}{\partial y} + \mathrm{A}c_i \frac{\mathrm{D}_i}{k\mathrm{T}} z_i e \frac{\partial \varphi}{\partial y}. \tag{3}$$

Including general cathodic reduction processes such as the reduction of quinone, involving consumption of quinone and hydrogen ions, we denote by s_i the number of mols of ions or molecules of type i which react in a cathodic process per one faraday F. A negative sign of s_i shall indicate that ions or molecules are evolved. Thus equation (3) for $y = 0$ becomes

$$\frac{dn_i}{dt} = \frac{s_i \mathrm{I}}{\mathrm{F}} = \mathrm{A}\mathrm{D}_i \left(\frac{\partial c_i}{\partial y}\right)_{y=0} + \mathrm{A}\frac{\mathrm{D}_i}{k\mathrm{T}} z_i e \left(c_i \frac{\partial \varphi}{\partial y}\right)_{y=0} \tag{4}$$

where I represents the strength of the electric current.

Upon multiplying each of the various equations (4) by z_i/D_i and adding, the sum of the terms involving the concentration gradients vanishes on account of the condition of electroneutrality

$$\Sigma z_i c_i = 0. \tag{5}$$

Thus the gradient of the potential at $y = 0$ becomes

$$\left(\frac{\partial \varphi}{\partial y}\right)_{y=0} = \frac{\mathrm{I}}{\mathrm{AF}} \cdot \frac{k\mathrm{T}}{e} \cdot \frac{\Sigma(z_i s_i/\mathrm{D}_i)}{\Sigma(z_i^2 c_i)_{y=0}}. \tag{6}$$

Upon introduction of equation (6) into one of the equations (4), referring to ions or molecules of type j, and solving for the concentration gradient, we obtain

$$\left(\frac{\partial c_j}{\partial y}\right)_{y=0} = \frac{I}{AF}\left[\frac{s_j}{D_j} - z_j c_j \frac{\Sigma(z_i s_i/D_i)}{\Sigma z_i^2 c_i}\right]_{y=0}. \tag{7}$$

This equation also holds true in the case of convection in the vicinity of the electrode because the velocity at the surface of the electrode vanishes.

For a particular case, we consider the electrolysis of a solution of copper sulfate containing a large excess of sulfuric acid. Assigning the subscripts 1, 2, and 3 to the ions Cu^{++}, H^+, and SO_4^{--} respectively, we have

$$\left.\begin{aligned} &z_1 = +2; \quad z_2 = +1; \quad z_3 = -2 \\ &c_1 \ll c_2 \leqq 2c_3 \\ &s_1 = \tfrac{1}{2}; \quad s_2 = 0; \quad s_3 = 0. \end{aligned}\right\} \tag{8}$$

Introduction into equation (7) yields

$$\left(\frac{\partial c_1}{\partial y}\right)_{y=0} \cong \frac{1}{2}\frac{I}{AFD_1} \tag{9}$$

$$\left(\frac{\partial c_2}{\partial y}\right)_{y=0} = \frac{I}{AFD_1}\left(-\frac{c_2}{4c_1 + c_2 + 4c_3}\right) \cong -\frac{1}{3}\frac{I}{AFD_1} \tag{10}$$

$$\left(\frac{\partial c_3}{\partial y}\right)_{y=0} = \frac{I}{AFD_1}\left(\frac{2c_3}{4c_1 + c_2 + 4c_3}\right) \cong \frac{1}{3}\frac{I}{AFD_1} \tag{11}$$

Substituting equation (9) in (10) and (11), we can eliminate the current I and obtain

$$\left(\frac{\partial c_2}{\partial y}\right)_{y=0} = -\frac{2}{3}\left(\frac{\partial c_1}{\partial y}\right)_{y=0} \tag{12}$$

$$\left(\frac{\partial c_3}{\partial y}\right)_{y=0} = +\frac{2}{3}\left(\frac{\partial c_1}{\partial y}\right)_{y=0}. \tag{13}$$

HYDRODYNAMIC EQUATIONS

As mentioned above, the solution near the cathode has a lower density than the bulk of the liquid, and accordingly an upward flow evolves in the vicinity of the cathode. The flow velocity equals zero at the surface, rises toward a maximum value, and decreases asymptotically to zero because the bulk of the liquid is presumed to be at rest. From the theory of one-dimensional diffusion in solids and liquids at rest, it is known that the "path of propagation" of a non-uniformity of concentration after a given time t is of the order $(Dt)^{\frac{1}{2}}$. If the average flow velocity in the boundary layer is denoted by v_a, a volume element passes the distance x from the lower edge of the cathode within the time x/v_a, and thus the path of propagation of a non-uniformity of concentration evolving at $x = 0$ is of the order $(D\,x/v_a)^{\frac{1}{2}}$.

The kinematic viscosity ν of a liquid can be interpreted as the diffusivity of momentum per unit volume in a given direction. Accordingly the path of propagation of a non-uniformity of momentum per unit volume evolving at $x = 0$ is of the order $(\nu t)^{\frac{1}{2}} \sim (\nu x/v_a)^{\frac{1}{2}}$.

Consequently, the ratio of the path of propagation of a non-uniformity of momentum to the path of propagation of a non-uniformity of concentration is of the order $(\nu/D)^{\frac{1}{2}}$, i.e., about H30 for the special case of aqueous solutions. In other words, the thickness of the hydrodynamic boundary layer is expected to be much greater than the thickness of the layer in which noticeable deviations from the bulk concentration occur.

After this qualitative exposition we approach the problem quantitatively. We refrain from the method used by E. Schmidt and W. Beckmann (6) for the corresponding heat transfer problem, but use an approximate method, first indicated by Th. von Kármán (7), for the latter method gives the main results in a far simpler manner.

According to von Kármán, the shearing stress at the surface of the cathode, given by the product of the dynamic viscosity μ and the gradient of the tangential flow velocity v, is to be equated to the sum of the integral of the buoyancy force extended over the boundary layer per unit surface and the increase of the flow of momentum per unit breadth per unit length in the flow direction. The latter term, however, can be disregarded in the case $\nu/D >> 1$ because the influence of friction is much greater than that of inertia, as can be shown with the aid of a tentatively assumed velocity distribution in the boundary layer. Thus,

$$\mu \left(\frac{\partial v}{\partial y}\right)_{y=0} \doteq -g \int_0^{\delta^*} \Delta\rho \cdot dy \tag{14}$$

where g represents the gravitational acceleration, $\Delta\rho$ the difference between the local density and the bulk density, and δ^* a distance beyond which the concentration differences and thus also $\Delta\rho$ practically vanish.

The density difference $\Delta\rho$ can approximately be written as a linear function of the concentration differences

$$\Delta\rho = \Sigma[c_i - c_{i(\omega)}]\rho_\omega \frac{\partial\, ln\, \rho}{\partial c_i} \tag{15}$$

where $c_{i(\omega)}$ represents the concentration of ions or molecules of type i in the bulk solution and ρ_ω the bulk density.

Upon introduction of equation (15) into (14), division by ρ_ω, and setting $\nu = \mu/\rho_\omega$, we obtain

$$\nu \left(\frac{\partial v}{\partial y}\right)_{y=0} = -g \int_0^{\delta^*} \Sigma\,[c_i - c_{i(\omega)}] \frac{\partial\, ln\, \rho}{\partial c_i} \cdot dy \tag{16}$$

We then consider the balance for each type j of the various molecules and ions in a volume element of the breadth b in the horizontal direction, the length dx in the vertical direction, and the thickness δ^*.

(a) The change per unit time at $y = \delta^*$ due to the migration of ions in the electrical field equals $(I/AF) \cdot (t_j/z_j) \cdot b \cdot dx$ mol/sec. where t_i represents the transference number and z_j the electrical valence.

(b) Diffusion at $y = \delta^*$ can be disregarded because it is assumed that practically all concentrations at $y = \delta^*$ equal the bulk concentrations.

(c) The flow velocity as well as the thickness of the boundary layer increases from bottom to top. Accordingly we have an inflow of solution at $y = \delta^*$ toward the cathode. The flow velocity v_n normal to the surface of the cathode can be obtained from the equation of continuity

$$\rho_o v_n = \frac{d}{dx}\int_0^{\delta^*} \rho v \cdot dy \cong \rho_o \frac{d}{dx}\int_0^{\delta^*} v \cdot dy. \tag{17}$$

Thus the quantity of ions and molecules passing per unit time into the volume element $b \cdot dx \cdot \delta^*$ corresponding to the flow velocity v_n at $y = \delta^*$ equals

$$c_{j(\infty)} v_n b \cdot dx = c_{j(\infty)} \cdot \left(\frac{d}{dx}\int_0^{\delta^*} v \cdot dy\right) b \cdot dx. \tag{18}$$

(d) The consumption at the cathode per unit time equals $(s_j\, \mathrm{I}/\mathrm{AF}) \cdot b \cdot dx$ according to equation (4).

(e) Next we consider the transport of ions and molecules due to the flow of the solution parallel to the cathode. The rate of ions or molecules entering the volume element $b \cdot dx \cdot \delta^*$ equals

$$\int_0^{\delta^*} v c_j b \cdot dy.$$

The loss per unit time is given by the difference of the rates at $x + dx$ and x and, therefore, equals

$$\left(\frac{d}{dx}\int_0^{\delta^*} v c_j b \cdot dy\right) \cdot dx.$$

Thus the balance for the component j at a steady state reads

$$\begin{aligned} \frac{\mathrm{I}}{\mathrm{AF}} \cdot \frac{t_j}{z_j} \cdot b \cdot dx + c_{j(\infty)} \left(\frac{d}{dx}\int_0^{\delta^*} v \cdot dy\right) b \cdot dx \\ - \frac{s_j \mathrm{I}}{\mathrm{AF}} \cdot b \cdot dx - \left(\frac{d}{dx}\int_0^{\delta^*} v c_j \cdot dy\right) b \cdot dx. \end{aligned} \tag{19}$$

Upon division by $b \cdot dx$ and rearrangement,

$$\frac{\mathrm{I}}{\mathrm{AF}} \cdot \left(\frac{t_j}{z_j} - s_j\right) - \frac{d}{dx}\int_0^{\delta^*} [c_j - c_{j(\infty)}] v \cdot dy = 0. \tag{20}$$

CALCULATION OF THE LIMITING DENSITY OF THE ELECTRICAL CURRENT

The above equations are not sufficient to obtain the concentrations c_j and the flow velocity v as functions of the coordinates x and y. According to von Kármán, however, we can introduce arbitrary plausible functions involving certain parameters which are to be determined from the above equations (7), (16), and (20), so that finally approximate representations of the values c_j and v result. It can be shown that the values of immediate

interest are fairly independent of the special form of the functions for c_i and v.

As mentioned above, the flow velocity v as a function of y rises from $v = 0$ at $y = 0$ to a maximum value v^* and then drops very slowly to zero. We are interested only in the first section and accordingly we introduce the following approximate representation

$$\left.\begin{aligned} v &= v^* \left[2\,\frac{y}{\delta_v} - \left(\frac{y}{\delta_v}\right)^2 \right] \quad \textit{for} \quad 0 \leqq y \leqq \delta_v \\ v &= v^* \quad \textit{for} \quad y \geqq \delta_v \end{aligned}\right\} \tag{21}$$

where v^* and δ_v are parameters, depending on x, which are to be determined below.

We also assume quadratic functions for the concentrations

$$c - c_{i(\infty)} = [c_i(y = 0) - c_{i(\infty)}] \left[1 - \frac{y}{\delta_i} \right]^2 \tag{22}$$

where $c_i(y = 0)$ and δ_i are further parameters, depending on x.

Let N denote the number of the independent components. If the current density is given, we have N equations (7), N equations (20), and equation (16), as a whole, $2N + 1$ equations involving N parameters $c_j(y = 0)$, N parameters δ_j, one parameter v^*, and one parameter δ_v. Thus the number of the unknowns exceeds the number of the equations by one. Therefore we have to introduce an additional assumption. In particular, we can equate the length δ_v in the velocity equation (21) to one of the values δ_i occurring in the equations (22). We would then be able to calculate the concentrations $c_i(y = 0)$ of the various components which determine the polarization of the cathode, if the current density were given. However, this type of problem has little practical bearing.

We then inquire into the limiting density of the current which occurs if the concentration of one of the components, e.g., $j = 1$ equals zero at $y = 0$. This condition can be realized in that the potential of the cathode is kept so low that practically all ions or molecules of type 1 arriving at the cathode are reduced immediately, and so high that no other reduction process, e.g., development of hydrogen, can take place. Thus equation (7) for $j = 1$ becomes

$$\left(\frac{\partial c_1}{\partial y}\right)_{y=0} = \frac{z_1}{\mathrm{FD}_1} \left(\frac{\mathrm{I}}{\mathrm{A}}\right)_x. \tag{23}$$

Conversely,

$$\left(\frac{\mathrm{I}}{\mathrm{A}}\right)_x = \frac{\mathrm{FD}_1}{z_1} \left(\frac{\partial c_1}{\partial y}\right)_{y=0}. \tag{24}$$

Here the subscript x indicates that the local current density at the distance x from the lower edge is to be taken into account.

Furthermore, we note that the transference number t_1 becomes negligible

$$t_1 \cong 0 \quad \textit{if} \quad c_1 \ll \Sigma z_i^2 c_i. \tag{25}$$

We then consider the special instance of the electrolysis of a copper sulfate solution containing a large excess of sulfuric acid. We confine our considerations to the concentrations of copper ions and hydrogen ions, from which the concentration of the sulfate ions can be derived by means of the principle of electroneutrality. Thus equation (22) for $j = 1$ with $c_1\ (y = 0) = 0$ becomes

$$c_1 - c_{1(\infty)} = -c_{1(\infty)} \cdot \left(1 - \frac{y}{\delta_1}\right)^2, \tag{26}$$

and for $j = 2$

$$c_2 - c_{2(\infty)} = [c_2(y = 0) - c_{2(\infty)}] \left(1 - \frac{y}{\delta_2}\right)^2. \tag{27}$$

Upon introduction of the expressions (26) and (27) into (12) and multiplication by $\delta_2/2$, we obtain

$$c_2(y = 0) - c_{2(\infty)} = \frac{2}{3} \frac{\delta_2}{\delta_1} c_{1(\infty)}. \tag{28}$$

Thus equation (27) becomes

$$c_2 - c_{2(\infty)} = \frac{2}{3} \frac{\delta_2}{\delta_1} c_{1(\infty)} \left(1 - \frac{y}{\delta_2}\right)^2. \tag{29}$$

According to the principle of electroneutrality, the concentrations of copper and hydrogen ions also determine the concentration of sulfate ions. Thus we can replace the derivatives of the density with respect to the concentrations of the various ions by the derivatives of the density with respect to electroneutral components. One gram ion of copper corresponds to one mol of copper sulfate, and one gram ion of hydrogen to half a mol of sulfuric acid. Thus

$$\Sigma[c_i - c_{i(\infty)}] \frac{\partial \ln \rho}{\partial c_i} = [c_1 - c_{1(\infty)}] \frac{\partial \ln \rho}{\partial c_{CuSO_4}} + [c_2 - c_{2(\infty)}] \frac{1}{2} \frac{\partial \ln \rho}{\partial c_{H_2SO_4}}. \tag{30}$$

Since the diffusion coefficient of hydrogen ions is greater than that of copper ions, it is to be expected that the non-uniformity of the hydrogen ion concentration extends to a greater distance than that of the copper ions. Consequently, the value δ_2 in equation (27) for the distribution of hydrogen ions must be greater than the value δ_1 for the distribution of copper ions in equation (26). Therefore we set the upper limit δ^* for the integrations equal to δ_2

$$\delta^* = \delta_2. \tag{31}$$

Since for $y > \delta_2$ all integrands in equations (16) and (20) vanish, the value of the integrals would be the same for any value $\delta^* > \delta_2$.

The flow velocity is caused by the density difference between the boundary layer and the bulk of the solution, and the density in turn depends on the concentration of copper sulfate rather than on the concentration of

sulfuric acid. Accordingly we equate the parameter δ_v to δ_1 and obtain instead of (21)

$$\left.\begin{aligned} v &= v^* \left[2\,\frac{y}{\delta_1} - \left(\frac{y}{\delta_1}\right)^2 \right] \quad for \quad 0 \leqq y \leqq \delta_1 \\ v &= v^* \quad for \quad \delta_1 \leqq y \leqq \delta_2 . \end{aligned}\right\} \tag{32}$$

Inserting the expressions (24), (25), (26), and (29) to (32) into (16) and (20) and setting

$$\delta_2 = \epsilon\delta_1 , \tag{33}$$

where ϵ denotes the ratio δ_2/δ_1, we obtain

$$\frac{2vv^*}{\delta_1} = g \int_0^{\delta_1} c_{1(o)} \left(1 - \frac{y}{\delta_1}\right)^2 \frac{\partial\, ln\, \rho}{\partial c_{CuSO_4}} \cdot dy - g \int_0^{\epsilon\delta_1} \frac{2}{3}\,\epsilon c_{1(o)} \left(1 - \frac{y}{\epsilon\delta_1}\right)^2 \frac{1}{2}\,\frac{\partial\, ln\, \rho}{\partial c_{H_2SO_4}} \cdot dy \tag{34}$$

$$-\frac{2c_{1(o)} D_1}{\delta_1} + \frac{d}{dx} \int_0^{\delta_1} c_{1(o)} \left(1 - \frac{y}{\delta_1}\right)^2 v^* \left[2\,\frac{y}{\delta_1} - \left(\frac{y}{\delta_1}\right)^2 \right] \cdot dy = 0 \tag{35}$$

$$\frac{4c_{1(o)} D_1 t_2}{\delta_1} - \frac{d}{dx} \int_0^{\delta_1} \frac{2}{3}\,\epsilon c_{1(o)} \left(1 - \frac{y}{\epsilon\delta_1}\right)^2 v^* \left[2\,\frac{y}{\delta_1} - \left(\frac{y}{\delta_1}\right)^2 \right] \cdot dy - \frac{d}{dx} \int_{\delta_1}^{\epsilon\delta_1} \frac{2}{3}\,\epsilon c_{1(o)} \left(1 - \frac{y}{\epsilon\delta_1}\right)^2 v^* \cdot dy = 0. \tag{36}$$

Integration yields

$$\frac{2vv^*}{\delta_1} = \frac{1}{3}\, g c_{1(o)}\, \delta_1 \left(\frac{\partial\, ln\, \rho}{\partial c_{CuSO_4}} - \frac{\epsilon^2}{3}\,\frac{\partial\, ln\, \rho}{\partial c_{H_2SO_4}} \right) \tag{37}$$

$$\frac{2c_{1(o)} D_1}{\delta_1} - \frac{2}{15}\, c_{1(o)}\, \frac{d(v^*\, \delta_1)}{dx} = 0 \tag{38}$$

$$\frac{4c_{1(o)} D_1 t_2}{\delta_1} - \frac{2}{3}\,\epsilon c_{1(o)} \left(\frac{\epsilon}{3} - \frac{1}{3} + \frac{1}{6\epsilon} - \frac{1}{30\epsilon^2} \right) \cdot \frac{d(v^*\, \delta_1)}{dx} = 0. \tag{39}$$

Upon elimination of $\partial(v^*\delta_1)/\partial x$ from (38) and (39),

$$\frac{2\epsilon}{3} \left(\frac{\epsilon}{3} - \frac{1}{3} + \frac{1}{6\epsilon} - \frac{1}{30\epsilon^2} \right) \frac{1}{2t_2} = \frac{2}{15}. \tag{40}$$

Numerical evaluation with $t_2 = 0.83$ as transference number of hydrogen ions in sulfuric acid yields

$$\epsilon = 1.41 \tag{41}$$

Inserting this value in equation (37) and solving for v^*, we have

$$v^* = \frac{g c_{1(o)}\, \delta_1^2}{6\nu} \left(\frac{\partial\, ln\, \rho}{\partial c_{CuSO_4}} - \frac{1.41^2}{3}\,\frac{\partial\, ln\, \rho}{\partial c_{H_2SO_4}} \right). \tag{42}$$

Introducing (42) into (38), integrating with $\delta_1 = 0$ for $x = 0$, and solving for δ_1, we obtain

$$\delta_1 = \left[\frac{120 D_1 \nu x}{g c_{1(\infty)} \left(\frac{\partial \ln \rho}{\partial c_{CuSO_4}} - \frac{1.41^2}{3} \frac{\partial \ln \rho}{\partial c_{H_2SO_4}} \right)} \right]^{\frac{1}{4}}. \tag{43}$$

Upon introduction of (43) into (42),

$$v^* = \left[\frac{10 D_1 g x c_{1(\infty)}}{3\nu} \left(\frac{\partial \ln \rho}{\partial c_{CuSO_4}} - \frac{1.41^2}{3} \frac{\partial \ln \rho}{\partial c_{H_2SO_4}} \right) \right]^{\frac{1}{2}}. \tag{44}$$

To illustrate, we calculate the numerical values of δ_1 and v^* for $x = 1$ cm. and $c_1 = 10^{-4}$mol/cm.^{3}, corresponding to a 0.1M copper sulfate solution, and obtain $\delta_1 = 2.7 \times 10^{-2}$ cm. and $v = 0.13$ cm./sec. If $x = 10$ cm., we obtain $\delta_1 = 4.9 \cdot 10^{-2}$ cm. and $v^* = 0.42$ cm./sec. It is to be pointed out that the value δ_1 represents the parameter involved in equation (22), whereas an "effective thickness of the boundary layer" is often calculated from measurements of the limiting current density under the assumption of a linear variation of the concentration throughout the whole boundary layer. According to equation (26), the gradient of the concentration at $y = 0$ equals $2c_{1(0)}/\delta_1 = c_{1(0)}/\frac{1}{2}\delta_1$ and thus the effective thickness of the boundary layer becomes $\frac{1}{2}\delta_1$.

Combining equation (24) with $s_1 = \frac{1}{2}$ and equations (26) and (43), we finally obtain the limiting current density

$$\left(\frac{I}{A}\right)_x = 2FD_1 \left(\frac{\partial c_1}{\partial y}\right)_{y=0} = \frac{4FD_1 c_{1(\infty)}}{\delta_1}$$
$$= 4FD_1 c_{1(\infty)} \left[\frac{g c_{1(\infty)}}{120 D_1 \nu x} \left(\frac{\partial \ln \rho}{\partial c_{CuSO_4}} - \frac{1.41^2}{3} \frac{\partial \ln \rho}{\partial c_{H_2SO_4}} \right) \right]^{\frac{1}{4}}. \tag{45}$$

Two points are significant. First, the limiting current density is inversely proportional to the 0.25th power of the distance x from the lower edge of the electrode where fresh solution enters the boundary layer. At greater distances x, the concentration deficit extends over a larger region; accordingly the thickness of the boundary layer increases and the limiting current density decreases.

Second, the limiting current density is proportional to the 1.25th power of the concentration $c_{1(\infty)}$. The greater this concentration, the greater is the density difference, the greater is the buoyancy force per unit volume, the greater is the flow velocity v^*, and accordingly the better is the supply of the ions consumed at the cathode. Therefore the parameter δ_1, characteristic of the thickness of the boundary layer, is inversely proportional to the 0.25th power of the concentration, and the limiting current density, which is proportional to $c_{1(0)}/\delta_1$, is consequently proportional to the 1.25th power of the concentration.

In general, the average limiting current density at an electrode of a given height H is observed. Averaging the expression (45), we have

$$\left(\frac{I}{A}\right)_H = \frac{1}{H} \int_0^H \left(\frac{I}{A}\right)_x \cdot dx$$
$$= \frac{16FD_1 c_{1(\infty)}}{3} \left[\frac{g c_{1(\infty)}}{120 D_1 \nu H} \left(\frac{\partial \ln \rho}{\partial c_{CuSO_4}} - \frac{1.41^2}{3} \frac{\partial \ln \rho}{\partial c_{H_2SO_4}} \right) \right]^{\frac{1}{4}}. \tag{46}$$

The results thus obtained are essentially analogous to the relations of the corresponding heat transfer problem. Yet the calculations of the electrochemical problem involve additional complications if the solution contains several components with individual contributions to the density difference between boundary layer and the bulk of the solution.

In the preceding exposition, only density differences due to the variations of the concentrations are taken into account. Tacitly the effect of eventual temperature differences is disregarded. Auxiliary calculations show that at a concentration of 0.1 mol per liter and a heat production of 23 kg.-cal. per gram equivalent ($\sim$ 1 electron volt) the temperature of the electrode is less than 1°C. above that of the electrolyte, and the resulting change of the density is much less than the change of the density due to variations of the concentrations.

EXPERIMENTAL

Experiments were carried out with a solution containing 0.1 mol copper sulfate and 1.0 mol sulfuric acid per liter. Both the cathode and the anode were copper. The backsides were covered with lacquer. In the first run, copper sheets with a breadth of 2 cm. and heights of 1, 4, and 16 cm. respectively were used. A practically constant voltage was furnished by a low-resistance potentiometer. In the range from 0.4 to 0.6 volt the current was practically independent of the voltage in accordance with above theoretical considerations. Cathodic development of hydrogen took place only at voltages greater than 0.6 volt. The observed current densities are compiled in Table I and are contrasted to values calculated from equation (46). The following numerical values, referring to 25°C. were used. $D_1 = 0.5 \cdot 10^{-5}$ cm.^{2}/sec.; $\nu = 0.011$ cm.^{2}/sec.; $\partial \ln \rho / \partial c_{CuSO4} = 0.166 \cdot 10^3$ (mol/cm.^{3})$^{-1}$; $\partial \ln \rho / \partial c_{H2SO4} = 0.068 \cdot 10^3$ (mol/cm.^{3})$^{-1}$.

TABLE I. *Limiting current densities at copper cathodes in 0.1M $CuSO_4$ + 1.0M H_2SO_4 at 25°C.*

H cm.	$(I/A)_H$	
	Observed	Calculated
1	0.0103	0.0094
4	0.0067	0.0066
16	0.0052	0.0047

The decrease of the average current density with increasing height of the electrode corresponds quantitatively to the theoretical formula (46). Moreover, the amount of the observed current densities are rather close to the calculated values, although the theoretical calculations involve great simplifications such as the introduction of arbitrary functions for the representation of the velocity and the concentrations in the boundary layer.

Deviations from the vertical position of the electrode up to 15 degrees had no noticeable effect.

Further tests were performed with a cathode consisting of five sections,

electrically isolated from each other, so that the current density of each section could be measured separately. The heights of the individual sections amounted to 1, 3, 1, 7, and 1 cm. respectively; thus the total height was 13 cm. Results compiled in Table II show the decrease of the local current density with increasing distance from the lower edge of the composite electrode. The observed current densities are as 1:0.62:0.56: 0.46:0.42, whereas the theoretical values, calculated by integration of equation (45) for each section, are as 1:0.61:0.51:0.44:0.40.

In addition, the interference between the sections of the composite electrode was investigated. Table III shows the current densities which were observed when either voltage was applied to one section only, or additionally to the lower or the upper section. The current density was

TABLE II. *Limiting current densities at a composite electrode in 0.1M $CuSO_4$ + 1.0M H_2SO_4 at 25°C.*

Electrode No.	Covered distance x from the lower edge of the composite electrode cm.	I/A amp./cm.^{2}
I	0 to 1	0.0100
II	1 to 4	0.0062
III	4 to 5	0.0056
IV	5 to 12	0.0046
V	12 to 13	0.0042

TABLE III. *Interference between the sections of a composite electrode*

(Temperature 25°C.)

Electrode No.	Covered distance x cm.	I/A(amp./cm.^{2}) if voltage is applied		
		To one section only	To one section and the adjacent upper section	To one section and the adjacent lower section
I	0 to 1	0.0102	0.0100	—
II	1 to 4	0.0073	0.0071	0.0063
III	4 to 5	0.0106	0.0104	0.0059
IV	5 to 12	0.0059	0.0059	0.0051
V	12 to 13	0.0094	—	0.0046

essentially independent of the conditions at the upper section, but the current density decreased when voltage was applied to the adjacent lower section, the average thickness of the boundary layer becoming greater in accordance with equation (43).

In a subsequent run the increase of convection due to the development of hydrogen was investigated. To this end an electrode consisting of two sections was used. The current flowing across the lower section with a height of 4 cm. was varied between 0 and 0.08 amp., and a voltage of 0.5 volt was applied to the upper section with a height of 1 cm. Results are compiled in Table IV. As long as the current flowing across the lower section was so small ($\sim$ 0.030 amp.) that only copper was deposited, the current density of the upper section decreased with increasing current of

the lower section in accordance with the results indicated above. When the current of the lower section exceeded 0.030 amp., copper as well as hydrogen ions were reduced and the current density of the upper section rose considerably. Under these conditions the readings of the current of the upper section were somewhat disturbed by irregular fluctuations. Obviously the ascending hydrogen bubbles increased the convection. Yet it is remarkable that the ascending hydrogen bubbles increase the limiting current density no more than by a factor of two. This observation shows that natural convection alone is relatively effective and forced convection becomes significant only when its intensity is fairly great.

Tests with copper sulfate concentrations greater or less than 0.1M were not so satisfactory. When a concentration of 0.5M was used, the surface of the copper deposit was rough so that flow conditions were less definite and thus results were less reproducible. Subsequent tests with a concentration of 0.02M also gave less reproducible results, possibly because of the smaller density difference between the boundary layer and the bulk of the solution.

TABLE IV. *Increase of convection due to ascending hydrogen bubbles*
(Temperature 15°C.)

Current at the lower section from $x = 0$ to $x = 4$ cm. amp.	Current density at the upper section from $x = 4$ cm. to $x = 5$ cm. amp./cm.^{2}
0.000	-0.0085
0.010	0.0083
0.020	0.0067
0.030	0.0067
0.040	0.0084
0.050	0.0102
0.060	0.012
0.070	0.013
0.080	0.014

CONCLUSIONS

In the theory herein developed, arbitrary but plausible functions for the velocity and the concentrations as functions of the distance y from the cathode have been introduced. A stricter method would consist in the discussion of the differential equations of the boundary layer. The partial differential equations resulting therefrom can be reduced to ordinary differential equations in the same manner as in the paper by E. Schmidt and W. Beckmann (6) which deals with the corresponding heat transfer problem. It can be shown that the general form of the equation (45) for the local limiting current density is

$$\left(\frac{I}{A}\right)_x = \frac{2FD_1 c_{1(o)}}{s_1}\left[\frac{g c_{1(o)}}{120 D_1 \nu x}\,\Sigma C_i \frac{\partial\, ln\, \rho}{\partial c_i}\right]^{\frac{1}{4}}. \qquad (47)$$

The dimensionless constants C_i of the order of unity are to be calculated from the solutions of the ordinary differential equations which, however, can be integrated only by cumbersome computations.

From a practical point of view it seems reasonable to calculate the expression $\Sigma C_i \partial \ln \rho / \partial c_i$ from equation (47) or the corresponding integrated form upon introduction of a measured value of the limiting current density. Thus a formula for a solution of a given composition is readily obtained. But it must be borne in mind that the expression $\Sigma C_i \partial \ln \rho / \partial c_i$ depends on the values s_i and z_i, the transference numbers t_i, and accordingly on the ratio of the various constituents of the solution.

In the preceding considerations it is assumed that the density of the boundary layer is less than that of the bulk of the solution. This is the case in most cathodic processes. But the theory can easily be extended to reactions involving an increase of density. Then a downward flow occurs and the distance from the upper edge of the electrode appears in all equations.

In the same manner, anodic processes can be treated.

The phenomenon of natural convection at vertical electrodes is of great practical bearing because otherwise no technical process could be performed without stirring. For example, we can calculate from equations given by H. J. S. Sand (8) that in 0.1M copper sulfate + 1.0M sulfuric acid a current density of 0.01 amp./cm.^{2} without hydrogen development can be maintained for only five seconds if no convection takes place, after which time the diffusion rate of copper ions over a steadily increasing distance is less than the equivalent of a current density of 0.01 amp./cm.^{2} In the case of a current density of 0.003 amp./cm.^{2}, the limiting time would be 47 sec.

In addition, we may consider another problem. Let us assume an electrolytic process at a vertical electrode with a given current less than the limiting current. If the current is given, we can calculate the concentrations of the reactants at the electrode. The greater the distance from the lower edge, where the upward flow starts, the greater the deficit of the ions consumed at the electrode. The thus resulting deviations from the concentrations in the bulk of the solution cause a polarization, which, under certain conditions, can be calculated from Nernst's formula. Accordingly we have to expect a decrease of the local current density from below to above. Tentative calculations, however, show that, practically, this effect is insignificant. This conclusion was confirmed by an experiment with a composite electrode. The individual currents were measured by reflecting galvanometers indicating the voltages across resistors of 0.1 ohm which were in line with the individual sections of the electrode so that the distribution of the currents was practically undisturbed by the measuring devices.

Any discussion of this paper will appear in the discussion section of Volume 95 of the TRANSACTIONS of the Society.

REFERENCES

1. H. F. WEBER, *Wiedemann's Ann. Physik*, **7**, 469, 536 (1879).
2. S. R. MILNER, *Phil. Mag.*, (6) **9**, 645 (1905).
3. R. E. WILSON AND M. A. YOUTZ, *Ind. Eng. Chem.*, **15**, 603 (1923).
4. S. GLASSTONE, *Trans. Electrochem. Soc.*, **59**, 277 (1931); "An Introduction to Electrochemistry," pp. 448-52, D. Van Nostrand Co., New York (1932).
5. R. E. EDGEWORTH-JOHNSTON, *Trans. Electrochem. Soc.*, **59**, 285 (1931).
6. E. SCHMIDT AND W. BECKMANN, *Tech. Mech. u. Thermodynam. (Forsch.)*, **1**, 341, 391 (1930).
7. TH. VON KÁRMÁN, *Z. angew. Math. u. Mech.*, **1**, 233 (1921); NACA Technical Memorandum No. 1092 (1946).
8. H. J. S. SAND, *Z. physik. Chem.*, **35**, 641 (1901); *Phil. Mag.*, (6) **1**, 45 (1901).

THE BASIC SULFATES OF LEAD[1]

J. J. LANDER

Chemistry Division, Naval Research Laboratory, Washington, D. C.

ABSTRACT

The formulas for the basic sulfates of lead have been checked or established. The phase diagram for melts of PbO and $PbSO_4$ shows the compounds: $PbSO_4 \cdot 4PbO$, $PbSO_4 \cdot 2PbO$, and $PbSO_4 \cdot PbO$. A wet method of preparation leads to the compounds: $PbSO_4 \cdot 4PbO$, $PbSO_4 \cdot PbO$, and a hydrous compound tentatively assigned the formula: $PbSO_4 \cdot 3PbO \cdot H_2O$. X-ray methods of analysis support these formulas. X-ray diffraction patterns have been recorded for these compounds for use in identification work. The thermal decomposition products of $PbSO_4 \cdot 2PbO$ and the hydrous compound have been shown to be a mixture of $PbSO_4 \cdot 4PbO$ and $PbSO_4 \cdot PbO$ in each case.

INTRODUCTION

As one phase in an investigation for the purpose of obtaining knowledge of the factors which control the properties of the pastes and active materials in the manufacture of lead-acid cells, a study of the nature of the compounds which can be formed by reaction of lead monoxide and lead sulfate was made. Some of these compounds may be formed in the paste mixing and drying steps and might affect these processes as well as the forming step and the properties of the formed plate.

Previous work has been done to determine the chemical formulas for these compounds. Jaeger and Germs (1) and Schenck (2) made thermal analyses of the PbO-$PbSO_4$ system and reported formation of the compounds $PbSO_4 \cdot 3PbO$, $PbSO_4 \cdot 2PbO$, and $PbSO_4 \cdot PbO$. They showed that the dibasic compound was unstable below 450°C. and stated that it decomposed into a mixture of the tribasic and monobasic compounds. Clark, *et al.* (3) reported various wet methods of formation of $PbSO_4 \cdot 4PbO$, $PbSO_4 \cdot 3PbO$, and $PbSO_4 \cdot 2PbO$, and gave x-ray data for these compounds. These reports are evidently in conflict because, first, a decomposition temperature of 450°C. for the dibasic lead sulfate indicates that its preparation at temperatures considerably below this is unlikely, second, the existence of a tetrabasic lead sulfate should be indicated by the thermal diagram, and finally, since the monobasic compound is stable at ordinary temperatures, it might be expected that it could be prepared by wet methods. For these reasons and the fact that our preliminary work did not confirm the reported x-ray patterns, it was decided to make the wet method preparations in a systematic fashion, following the reactions by x-ray analysis, and also to check the thermal analysis.

THEORETICAL CONSIDERATIONS

X-ray analysis in conjunction with thermal analysis is a method frequently used to determine phase diagrams. This is possible because all

[1] Manuscript received December 1, 1948. This paper prepared for delivery before the Philadelphia Meeting, May 4 to 7, 1949.

crystalline compounds give characteristic powder patterns. Thus, diffraction patterns of a series of solidified melts with compositions ranging from pure A to pure B should show the existence of compounds and their approximate composition, since the intensities of the lines of the pattern for a compound should be greatest at the concentration where the compound should exist pure as indicated by the phase diagram. Similarly, if a series of mixtures of A and B ranging in composition from pure A to pure B are boiled in water suspension, compound formation should be indicated by the x-ray patterns of the resulting materials and the chemical formulas would be indicated by the compositions at which the lines of the characteristic patterns reached maximum intensities.

In general, solid compounds are most easily identified by their x-ray powder patterns, so that if compounds of PbO and $PbSO_4$ could be prepared in substantially pure form by the above methods, the diffraction patterns obtained for them could serve as a means of identification in preparations of battery pastes.

EXPERIMENTAL METHODS AND APPARATUS

Phase study.—For this work 100 to 130 gram mixtures of Baker's yellow lead monoxide of National Formulary quality and Merck's reagent quality lead sulfate, ranging in composition from pure PbO to a 50–50 mol per cent mixture were melted in a platinum crucible and allowed to cool at rates of 3° to 5° per minute. The melts were stirred continuously with a motor-driven stirrer made from 90 per cent platinum 10 per cent rhodium alloy thermocouple wire. The melts were usually seeded, since they had a pronounced tendency to supercool at inflections and arrests in spite of efficient stirring. Temperatures were measured by a platinum-platinum rhodium (10%) thermocouple immersed uninsulated in the melt. The potential as the melt cooled was recorded by a General Electric recorder. Potentials of inflections and arrests were checked with a Rubicon 150 millivolt portable potentiometer. The solidified melts from the phase study were used to obtain x-ray powder patterns.

Wet method of preparation.—Suspensions of about 10 gram mixtures of PbO and $PbSO_4$ in 2 to 3 liters of water were allowed to boil from 7 to 8 hours. The mixtures were then filtered and dried in an oven overnight at 75°C. before preparing samples for the x-ray analysis.

Sample preparation.—The crystals resulting from the melts were ground for about one-half hour by hand in a mortar. The resulting powder was pressed into a disc one inch (2.54 cm.) in diameter and about one-eighth inch (.32 cm.) thick and mounted on a glass slide and the x-ray diffraction pattern obtained. The same treatment, except for grinding, was given the dried powders from the wet method preparations. Grinding was unnecessary because the particle size was already very small and grinding for periods up to one-half hour resulted in no change in the pattern.

X-ray apparatus.—A North American Philips x-ray spectrometer with a modified silt system and counting circuit was used to obtain the powder patterns. A copper target x-ray tube operating on 35 kv. and 6.8 ma. was used for the source of radiation.

RESULTS

Phase study.—Table I gives the temperatures of inflections and arrests for the cooling curves at various compositions. Figure 1 presents the

TABLE I. *Data from the phase study*

$PbSO_4$ (Mol %)	Inflection (°C.)	Arrest (°C.)
0	—	878
10	853	834
11	860	835
13	878	835
15	888	835
17	895	832
18	893	830
19	893	820
20	899	895
21	903	895
22	915	895
24	928	895
25	940	895
26	945	893
28	954	892
29	956	888
31	960	886
33	—	961
37	957	950
39	—	950
45	972	950
50	—	975

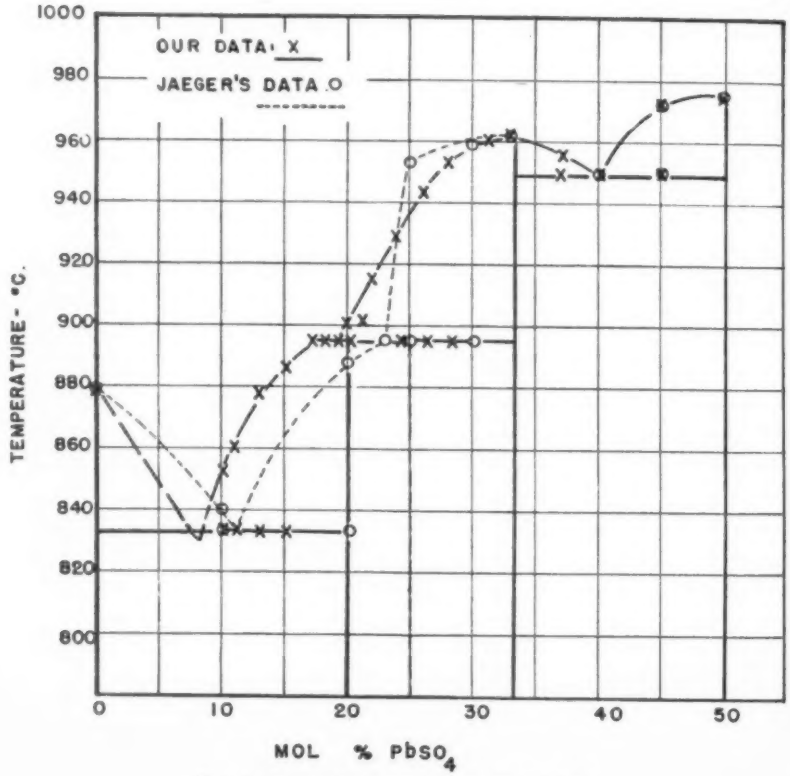

FIG. 1. Phase diagram: System PbO-$PbSO_4$

phase diagram obtained from the cooling curves and compares it with the diagram obtained by Jaeger. Except for the range between 10 and 27 mol per cent, these data check Jaeger's very well; however they definitely show the existence of a tetrabasic rather than a tribasic lead sulfate. The

TABLE II. *X-ray data on compounds prepared by dry method*
(Intensities relative to strongest line of pattern)

Pure PbO*		20 mol % $PbSO_4$		33⅓ mol % $PbSO_4$		50 mol % $PbSO_4$	
d	I	d	I	d	I	d	I
5.8	.15	7.9	.11	7.8	.10	6.1	.02
4.9	.06	3.22	1.00	5.8	.10	5.8	.10
3.04	.11	3.09	.15	3.75	.05	4.4	.01
2.92	1.00	3.04	.11	3.47	.10	3.68	.01
2.79	.06	2.92	.13	3.22	.60	3.47	.01
2.50	.40	2.87	.20	2.96	1.00	3.32	.10
1.99	.06	2.66	.20	2.92	1.00	3.16	.03
1.96	.30	2.30	.11	2.87	.70	2.93	1.00
1.86	.05	2.04	.11	2.69	.05	2.84	.10
1.85	.02	1.94	.19	2.37	.50	2.46	.02
1.71	.08	1.86	.11	2.35	.50	2.42	.02
1.63	.02	1.82	.13	2.29	.10	2.33	.02
1.52	.05	1.72	.18	2.22	.05	2.26	.04
1.46	.35	1.68	.15	2.11	.15	2.21	.06
1.287	.02	1.64	.17	2.06	.20	2.05	.08
1.251	.04	1.61	.21	1.96	.40	1.96	.50
1.173	.06	1.59	.15	1.89	.05	1.90	.01
		1.58	.15	1.86	.05	1.84	.10
		1.55	.05	1.82	.25	1.75	.06
		1.422	.05	1.79	.40	1.72	.05
		1.361	.11	1.74	.10	1.71	.04
		1.282	.12	1.73	.20	1.67	.01
		1.268	.17	1.68	.20	1.66	.01
		1.257	.12	1.62	.05	1.64	.02
		1.222	.08	1.56	.30	1.61	.02
		1.155	.12	1.52	.20	1.60	.01
				1.51	.10	1.51	.11
				1.44	.10	1.49	.01
				1.426	.06	1.47	.08
				1.329	.02	1.445	.04
				1.316	.02	1.435	.07
				1.298	.02	1.352	.01
				1.245	.05	1.305	.02
				1.235	.05	1.281	.02
				1.210	.02	1.228	.01
				1.178	.02	1.210	.02
				1.167	.20	1.177	.08
						1.169	.04
						1.151	.01
						1.133	.01

* This is a mixture of the tetragonal and orthorhombic forms.

reason for this disagreement is not apparent. Both sets of data show compound formation at 33⅓ per cent and 50 per cent, and the temperatures of inflections and arrests check within one or two degrees centigrade. The dibasic compound has an arrest at 450°C., as found by Jaeger, which is not

indicated on the figure or in the table. This arrest results from decomposition of the dibasic compound into a mixture of mono- and tetrabasic lead sulfates as will be demonstrated later from the x-ray patterns.

X-ray data for compounds prepared from the melts.—The x-ray data for these compounds are given in Table II where line positions and relative intensities are given for the solids obtained from the following melts: pure PbO, 20 mol per cent $PbSO_4$, $33\frac{1}{3}$ mol per cent $PbSO_4$ and 50 mol per cent $PbSO_4$. Actually, patterns of solidified melts in steps of from one to five per cent, from pure PbO to 50 mol per cent $PbSO_4$, were examined. They showed compound formation at about 20, $33\frac{1}{3}$, and 50 mol per cent

TABLE III. *Intensity variations with $PbSO_4$ concentration of some strong lines of compounds formed in the melts*

d	Intensities in scale divisions									
	Concentration of $PbSO_4$ (mol %)									
	0	10	15	20	25	30	$33\frac{1}{3}$	35	40	50
5.8	7.5	4.0	1.0							
3.6									0.6	2.2
3.32								1.0	3.4	5.0
3.22		7+	7+	7+	7+	5.4	4.4	4.2	2.0	
3.11								1.0	1.2	2.0
2.96				3.0	7+	7+	7+	7+		
2.93							6.8	6.8	7+	7+
2.87		2	3.0	5.4	7+	7+	7+	7+	3.2	
2.66		2	3.4	3.8	2.6	1.0				
2.51	7+	7+	1.2							
2.42									0.6	2.0
2.37				0.8	1.4	4.3	4.2	2.0	0.4	
2.26								0.8	1.4	3.0
2.21							0.4	1.0	1.4	3.6
2.06				1.2	1.8	1.4	2.2	2.0		
2.05									4	4.6
1.86	2.8	1.8	0.8							
1.79					1.2	3.2	3.0	1.4	0.4	
1.64		0.3	1.6	2.2	1.0					
1.61			2.0	3.4	3.4	0.8				
1.56				0.4	0.4	2.4	2.4	2.0	0.6	
1.52	2.4	2	0.8							
1.44					0.6	1.2	3.0	1.6	0.8	3.6
1.268		0.6	1.2	1.4	0.8	0.4				
1.177								0.4	1.2	2.4
1.173	4.4	0.4								

$PbSO_4$. All the data are not included because of their cumbersome nature. Instead, in Table III the intensity values of several strong lines of each compound are given as a function of concentration of $PbSO_4$, which should be sufficient to illustrate the basis of the argument. Thus, the x-ray method places compound formation at about the same compositions as the thermal analysis and provides a check on the results. In this case, thermal analysis is the more exact method for locating these compositions.

The patterns for the compounds formed from the melts are not entirely pure, each being contaminated to a slight extent with other basic sulfates or PbO. This is particularly true for the dibasic compound. It is perhaps

to be expected because the mono- and the dibasic compounds are dissociated to some extent in the melt, while the tetrabasic compound is unstable below its melting point. Nevertheless, there are three distinct patterns other than pure PbO or $PbSO_4$ in the series, and the compositions for which the intensities of the lines of the pattern reach maximum are consistent

TABLE IV. *X-ray data on decomposed dibasic lead sulfate*
(Intensities relative to strongest line of pattern)

Decomposition product		Matching lines from:	
		Tetrabasic	Monobasic
d	I	d	d
6.1	.14		6.1
5.8	.07		5.8
4.4	.03		4.4
3.69	.03		3.68
3.32	.85		3.32
3.22	1.00	3.22	
3.18	.20		3.16
3.10	.60	3.09	
3.03	.70	3.04	
2.94	1.00		2.93
2.87	0.70	2.87	
2.65	0.60	2.66	
2.58	.12		2.46
2.46	.12		2.42
2.41	.10		2.33
2.33	.05		2.26
2.26	.20		
2.11	.05		
2.05	.40	2.04	2.05
1.97	.30		1.96
1.94	.50	1.94	
1.84	.30		1.84
1.76	.10		1.75
1.72	.20	1.72	1.72
1.67	.15	1.68	1.67
1.64	.20	1.64	
1.61	.10	1.61	1.61
1.60	.10	1.59	1.60
1.57	.10		
1.55	.05	1.55	1.51
1.51	.05		
1.43	.08	1.422	1.435
1.345	.02		1.352
1.267	.08	1.268	

with the compositions for compound formation shown by the phase diagram.

Decomposition of the dibasic compound into a mixture of tetrabasic and monobasic lead sulfates is shown by Table IV, where are given the x-ray data for a sample of the dibasic which had been held at a temperature of 410°C. for thirty-six hours. The d values for the decomposition product are given in Table IV along with a comparison with matching values for the tetra- and monobasic lead sulfates.

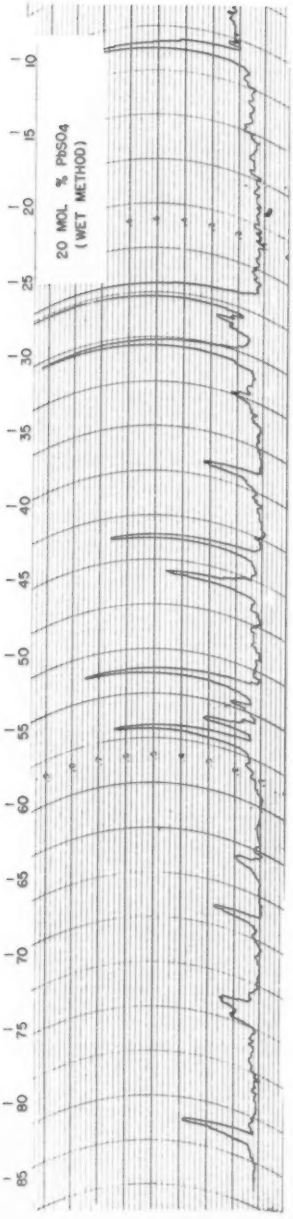
20 MOL. % PbSO4
(WET METHOD)

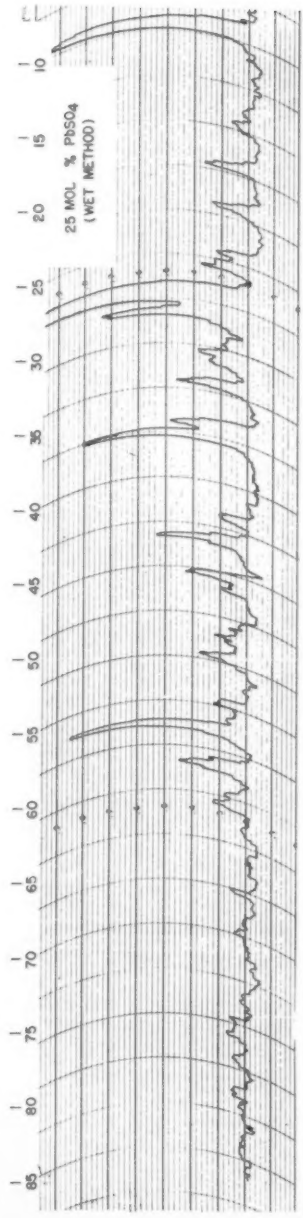
25 MOL. % PbSO4
(WET METHOD)

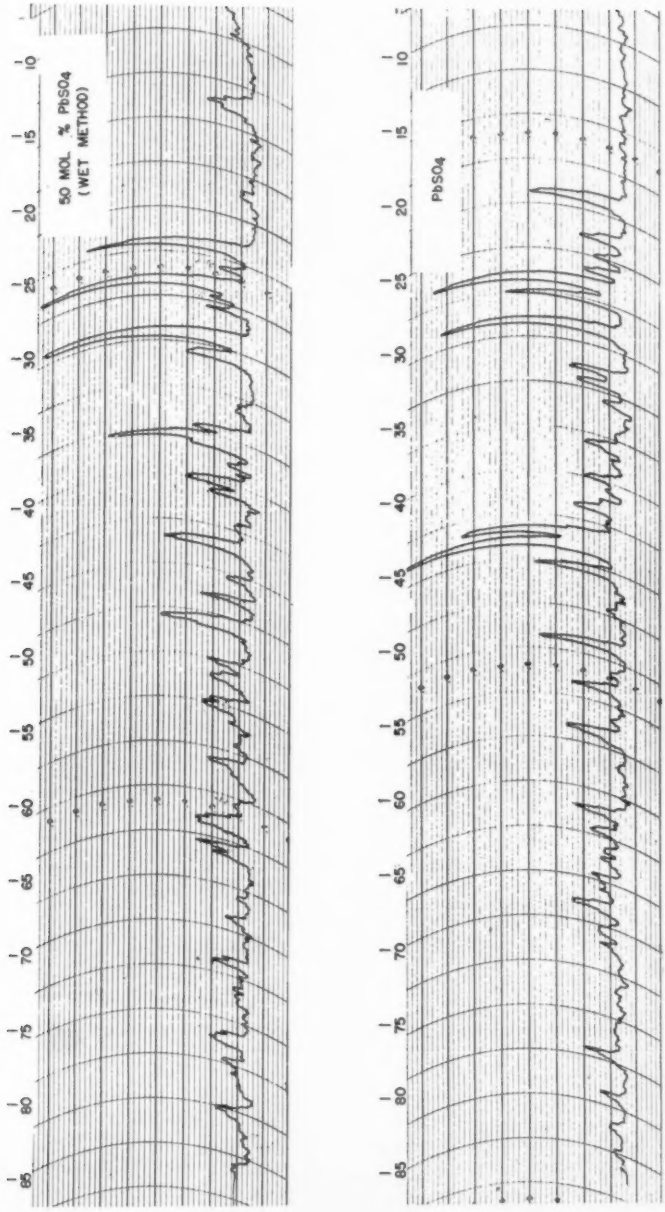

FIG. 2. Patterns for Compounds Prepared by the Wet Method

X-ray data for compounds prepared by the wet method.—Patterns for compounds prepared by this method seem to be purer as was shown by the sharpness of the transitions and lack of persistence of lines in ranges where they should not be. Examination of the patterns in 5 per cent steps from pure PbO to pure $PbSO_4$ showed compound formation at 20, 25, and 50 mol per cent $PbSO_4$. The x-ray data for these compounds are given in Table V. Table VI gives the intensity values for strong lines as a function of concentration. A photograph of these patterns is shown in Fig. 2 as an example of the patterns obtained.

TABLE V. *X ray data on compounds prepared by the wet method*
(Intensities relative to strongest line of pattern)

20 mol % $PbSO_4$		25 mol % $PbSO_4$		50 mol % $PbSO_4$		Pure $PbSO_4$		Hannawalt Index on $PbSO_4$	
d	I	d	I	d	I	d	I	d	I
8.1	.30	9.8	.3	6.2	.2	4.20	0.44	4.26	0.80
3.25	1.00	6.1	.02	5.8	.1	3.82	0.22	3.80	0.28
3.11	.03	5.8	.02	4.4	.02	3.59	0.18	3.61	0.08
3.04	.02	4.85	.08	3.67	.80	3.44	0.20	3.47	0.08
2.87	.30	4.24	.08	3.47	.10	3.31	0.88	3.33	0.60
2.67	.02	3.68	.07	3.33	1.00	3.20	0.56	3.21	0.40
2.31	.10	3.54	.10	3.22	.10	2.99	0.85	3.00	1.00
2.04	.20	3.27	1.00	3.16	.10	2.74	0.25	2.75	0.32
1.94	.15	3.12	.20	2.95	1.00	2.68	0.22	2.68	0.32
1.72	.25	2.96	.02	2.84	.30	2.61	0.10		
1.68	.02	2.92	.02	2.57	.05	2.39	0.20	2.40	0.12
1.64	.08	2.88	.08	2.46	.25	2.25	0.20	2.27	0.12
1.61	.20	2.82	.08	2.42	.70	2.22	0.08		
1.437	.08	2.69	.10	2.39	.25	2.19	0.10		
1.364	.08	2.49	.10	2.34	.05	2.16	0.22	2.16	0.16
1.345	.01	2.44	.22	2.26	.12	2.06	0.69	2.06	1.00
1.269	.08	2.21	.01	2.22	.10	2.03	1.00	2.02	0.40
1.255	.06	2.14	.08	2.11	.05	1.97	0.40	1.97	0.20
1.156	.20	2.07	.15	2.05	.40	1.87	0.08	1.87	0.04
		1.97	.10	1.96	.12	1.79	0.40	1.78	0.12
		1.94	.05	1.91	.15	1.74	0.06	1.73	0.06
		1.84	.05	1.84	.50	1.70	0.25	1.70	0.12
		1.81	.05	1.76	.10	1.64	0.05	1.65	0.04
		1.77	.08	1.72	.10	1.62	0.30	1.61	0.20
		1.68	.06	1.67	.15	1.57	0.02	1.57	0.04
		1.63	.25	1.66	.15	1.49	0.25	1.490	0.16
		1.57	.10	1.64	.05	1.465	0.15		
		1.53	.05	1.57	.20	1.435	0.10		
		1.51	.06	1.51	.05	1.427	0.10		
		1.394	.05	1.48	.20	1.401	0.10		
		1.354	.02	1.47	.20	1.390	0.08		
		1.255	.05	1.445	.20	1.366	0.20		
		1.248	.05	1.435	.15	1.338	0.08		
		1.218	.03	1.380	.02	1.324	0.06		
		1.192	.03	1.360	.05	1.220	0.20		
				1.306	.10	1.182	0.15		
				1.232	.10	1.162	0.10		
				1.213	.05	1.143	0.08		
				1.174	.10				

A comparison of the 20 per cent and 50 per cent patterns for the same

TABLE VI. *Intensity variations with $PbSO_4$ concentration of some strong lines of compounds formed from the wet method*

	Intensities in scale divisions									
	Concentration of $PbSO_4$ (mol %)									
d	0	10	15	20	22	25	30	40	45	50
9.8					9+	9+	9+	9+	9+	
8.1		3.4	5.4	9	2.4					
6.2								1	1.6	2.0
5.0	8	1.8	0.8							
4.85					1.0	1.6	3.0	1.6	1.6	
3.54					1.0	2.0	2.0			
3.27					9+	9+	9+	9+	9+	1.6
3.25		9+	9+	9+						
3.11	9+	5.8	4.4	1.0	1.4	4.0	4.0	2	1.4	
2.95							1.8	2.4	3.0	5.4
2.87		4.2	6.2	7.2	5.4	1.8				
2.69					1.4	2.0	2.0	1.2	0.8	
2.51	9+	9+	9							
2.44					4.2	9+	9+	8.0	4.0	
2.31		0.8	1.4	1.8	1.0	0.2				
2.26							0.4	1.0	1.4	2.0
2.22							0.4	0.6	0.8	1.4
1.87	3.4	2.2	0.8							
1.72		3.4	4.0	5.8	3.4	2.4	0.4			
1.63		0.2	1.0	1.6	5.0	9+	9+	8	6	
1.61		2.2	2.6	4.0	2.6	2.6				
1.55	5.4	3.0	1.4							
1.436		0.8	1.0	1.0	0.6	0.4		0.2	0.6	1.0
1.364		0.2	0.6	1.2	0.4	0.2				
1.156		0.2	1.2	1.8	1.0	0.4				

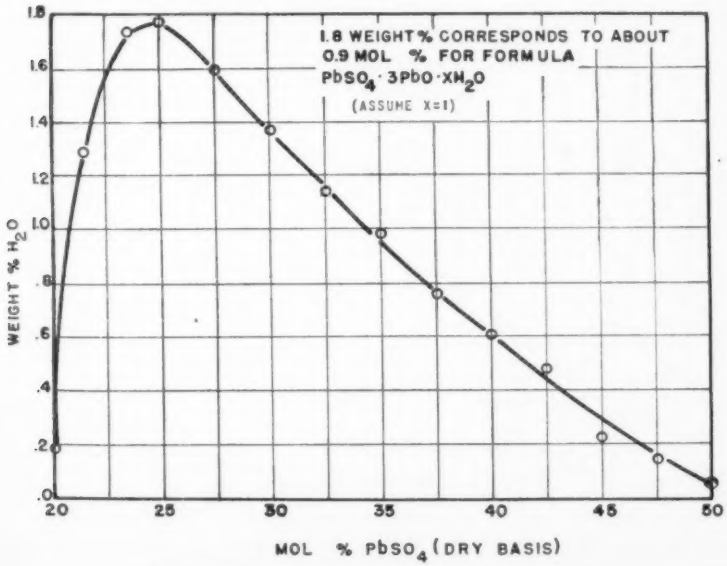

FIG. 3. Water content of wet method samples

compositions from the melt shows excellent correspondence of line positions. The fact that maximum intensities for these two patterns occur very near 20 and 50 per cent coincides nicely with the thermal data and the x-ray data on the solidified melts.

The composition of the compound which occurs at 25 per cent $PbSO_4$ is not known with certainty. It is probably a hydrate because it loses water in heating above about 210°C. A quantitative analysis for water loss of all samples from 20 to 50 per cent was made and the results are graphed in Figure 3. Maximum water loss occurs at 25 mol per cent $PbSO_4$, but the amount lost is about 10 per cent less than the theoretical amount for a monohydrate of tribasic lead sulfate ($PbSO_4 \cdot 3PbO \cdot H_2O$). There-

TABLE VII. *X-ray data for decomposed hydrous compound*

Decomposition product		Matching lines from:	
		Tetrabasic	Monobasic
d	I	d	d
3.68	.05		3.68
3.33	1.00		3.33
3.22	.30	3.22	
3.10	.30	3.09	
3.04	.30	3.04	
2.94	.10		2.93
2.86	.10	2.87	
2.72	.10		
2.67	.20	2.67	
2.60	.05		
2.55	.05		2.57
2.42	.05		2.42
2.28	.05		2.26
2.12	.02		2.11
1.99	.05		
1.96	.10		1.96
1.94	.15	1.94	
1.85	.15	1.86	1.84
1.71	.10	1.72	1.71
1.68	.02	1.68	1.67
1.65	.10	1.64	1.66
1.61	.10	1.61	1.61
1.57	.02	1.58	
1.53	.02	1.53	1.51
1.48	.05		1.47

fore this compound will be referred to by that name tentatively only. When it breaks down under heating, it forms a mixture of the mono- and tetrabasic lead sulfates. This might be expected since the phase diagram does not show the existence of a tribasic lead sulfate. The x-ray data are tabulated in Table VII. As is to be expected, the dibasic lead sulfate is not formed by the wet method, since there was no corresponding change in the patterns of the series at $33\frac{1}{3}$ mol per cent $PbSO_4$.

DISCUSSION

In view of the methods used to produce these compounds, there is no absolute guarantee that the melts and the boiled suspensions gave pure

compounds at the concentrations which should correspond to compound formation. Consequently, the possibility of assigning lines incorrectly to a pattern for a given compound must not be overlooked; however, from a study of the intensity variations in the lines as concentration is changed, d values should be assignable to the pattern of any one compound, for the most part with accuracy unless they are rather weak lines. The intensity variations in the patterns of the boiled suspensions are so clean cut that it is probable that the patterns recorded for those samples represent

TABLE VIII. *Characteristic X-ray data for the basic sulfates of lead*

Tetrabasic lead sulfate		Hydrous compound		Dibasic lead sulfate		Monobasic lead sulfate	
d	I	d	I	d	I	d	I
8.1	.30	9.8	.30	3.75	.05	6.2	.20
3.25	1.00	4.85	.08	2.96	1.00	5.8	.10
3.11	.03	4.24	.08	2.87	.70	4.4	.02
3.04	.02	3.54	.10	2.69	.05	3.67	.80
2.87	.30	3.27	1.00	2.37	.50	3.47	.10
2.67	.02	3.12	.20	2.35	.50	3.33	1.00
2.31	.10	2.82	.08	2.29	.10	3.16	.10
2.04	.20	2.69	.10	2.11	.15	2.95	1.00
1.94	.15	2.49	.10	2.06	.20	2.84	.30
1.86	.11	2.44	.22	1.96	.40	2.46	.25
1.72	.25	2.21	.01	1.82	.25	2.42	.70
1.68	.02	2.14	.08	1.79	.40	2.39	.25
1.64	.08	2.07	.15	1.74	.10	2.34	.05
1.61	.20	1.97	.10	1.73	.20	2.26	.12
1.59	.15	1.77	.08	1.68	.20	2.22	.10
1.58	.15	1.68	.06	1.56	.30	2.05	.40
1.437	.05	1.63	.25	1.52	.20	1.96	.12
1.364	.08	1.57	.10	1.426	.06	1.91	.15
1.269	.08	1.51	.06	1.245	.05	1.84	.50
1.255	.06	1.394	.02	1.235	.05	1.76	.10
1.156	.20	1.345	.02	1.167	.20	1.72	.10
		1.255	.05			1.67	.15
		1.248	.05			1.66	.15
		1.218	.03			1.64	.05
		1.192	.03			1.57	.20
						1.51	.05
						1.48	.20
						1.47	.20
						1.445	.20
						1.435	.15
						1.360	.05
						1.306	.10
						1.232	.10
						1.213	.05
						1.174	.10

substantially pure compounds. Furthermore, superposition of the patterns of the mono- and tetrabasic lead sulfates obtained from the melt upon the corresponding patterns from the boiled suspensions showed excellent correspondence in each case. There is considerable variation in relative intensities which might be ascribed to either the method of sample preparation, or the method of making the compounds, or both.

It should be pointed out that the complete answer to this problem of pure patterns awaits the structure determinations for these compounds

unless some independent guide for purity could be found. As the situation now exists, the x-ray patterns for the compounds prepared by the wet method furnish the best comparison for judging the purity of subsequent preparations of these compounds.

The patterns for any given method of preparation of compound and sample are quite reproducible. Most of them have been recorded two or three times from different preparations of the same composition by the same method, and only minor variations in intensities and variation in d values within the limits of experimental error were observed.

SUMMARY

1. Three compounds may be formed by melting PbO and $PbSO_4$ in the ratios indicated by their formulas: $PbSO_4 \cdot 4PbO$, $PbSO_4 \cdot 2PbO$, and $PbSO_4 \cdot PbO$. Dibasic lead sulfate is unstable below 450°C. and decomposes into a mixture of the tetra- and monobasic lead sulfates.

2. Three compounds may be formed by boiling water suspensions of PbO and $PbSO_4$ in the proper ratio. Two of these are assigned the formulas: $PbSO_4 \cdot 4PbO$ and $PbSO_4 \cdot PbO$. The third compound seems to be a hydrate and on the basis of the available data is tentatively assigned the formula $PbSO_4 \cdot 3PbO \cdot H_2O$. This compound decomposes on heating at about 210°C. into a mixture of the tetra- and monobasic lead sulfates.

3. The d values of the lines considered to be characteristic of the patterns of these compounds are tabulated in Table VIII, together with their relative intensities, as recorded for the patterns for those samples prepared by the wet method, except for the dibasic lead sulfate, where the pattern for the sample from the melt must be used.

ACKNOWLEDGMENT

Permission of the Naval Research Laboratory to publish this work is gratefully acknowledged by the author.

Any discussion of this paper will appear in the discussion section of Volume 95 of the TRANSACTIONS of the Society.

REFERENCES

1. F. M. JAEGER AND H. C. GERMS, *Z. anorg. u. allgem. Chem.*, **119**, 145–173 (1921).
2. R. SCHENCK, *Metall u. Erz*, **23**, 408–420 (1926).
3. G. L. CLARK, J. N. MRGUDICH, AND N. C. SCHIELTZ, *Z. anorg. u. allgem. Chem.*, **229**, 401–409 (1936).

CALCIUM HALOPHOSPHATE PHOSPHORS[1]

RUDOLPH NAGY, R. W. WOLLENTIN, AND C. K. LUI

Research Department, Westinghouse Electric Corporation, Bloomfield, New Jersey

ABSTRACT

Calcium halophosphates were prepared by firing together calcium chloride and calcium fluoride in various ratios with calcium phosphate containing antimony and manganese as activators, in an electric furnace at 1060°C. for 1 hour. The x-ray diffraction studies gave patterns very similar to the mineral apatite. Spectral energy distribution measurements indicated that as the chlorine was replaced by equal mole fractions of fluorine, the peak of emission shifted from 5800 Å for all chlorine to 5550 Å when only fluorine was used. Calcium halophosphate activated with antimony alone has a peak of fluorescence at about 4800 Å. As the percentage of manganese is increased up to five per cent, the blue emission is entirely suppressed and a broad peak is obtained at about 5800 Å. The amount of antimony in the phosphor does not appreciably affect the fluorescent color. Excitation measurements of various calcium halophosphates reveal that there are two distinct peaks. A major one is located near 2500 Å and a minor one at 2200 Å. Replacing the chlorine by fluorine tends to shift the major peak toward the longer wavelengths. The effect of manganese seemed to be to enhance the minor excitation peak at 2200 Å. Fluorescent lamps made from this phosphor have been obtained that have outputs and color temperatures comparable to lamps made with zinc beryllium silicate and magnesium tungstate.

As part of a broad program in the study of new phosphors, calcium phosphate with various elements substituted for a portion of the calcium was investigated for its emission in various portions of the spectrum. One of the phosphors which was extensively studied was the calcium halophosphate having the apatite configuration.

The mineral apatite, which is mainly calcium phosphate with a small amount of calcium fluoride and chloride, has been known for a long time to fluoresce when exposed to 2537 Å radiation. Calcium halogen phosphate activated by manganese does not have appreciable fluorescence. McKeag and Ranby (1, 2, 3) have greatly improved the fluorescent output by adding a small amount of antimony in addition to the manganese. They have also reported that bismuth, tin, or lead could be used as activators in the halogen phosphates. Their work showed further that the spectral distribution could be shifted by varying the ratio of the chloride to the fluoride and by varying the amount of manganese. McKeag and Ranby (4) and Jenkins and McKeag (5) have indicated the magnitude of some of the effects of composition on the spectral energy distribution. Their interest in this phosphor was enhanced because of the scarcity of beryllia and tungsten in England and because of the advantage that a single component phosphor giving white light would offer in a fluorescent lamp.

[1] Manuscript received December 1, 1948. This paper prepared for delivery before the Columbus, Ohio, Meeting, April 14 to 17, 1948.

The recent improvement in output of British lamps has been mainly due to the use of such halophosphates. However, there has been no report in this country and very little from abroad which gives us an understanding of this phosphor group.

In view of the limited knowledge of the apatite phosphors and their theoretical and possible economic importance, a preliminary study of the effect of composition on the excitation and emission spectra has been undertaken.

EXPERIMENTAL

The apatite phosphor has the following general composition:

$$3Ca_3(PO_4)_2 \cdot CaClF \cdot (0 \text{ to } 5\%)Mn \cdot (1 \text{ to } 10\%)Sb$$

That is, for every three mols of calcium phosphate there is one mol of calcium halide. Increasing or decreasing the amount of calcium phosphate by more than ten mol per cent from the above ratio had a detrimental effect on the fluorescent output indicating that the apatite composition is

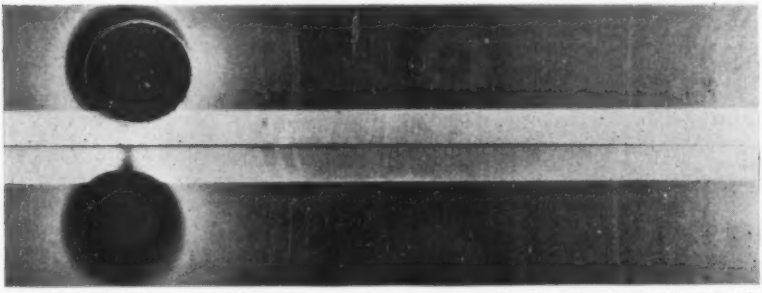

FIG. 1. X-ray diffraction patterns of calcium halo phosphate (top) and tricalcium phosphate (bottom), showing that the phosphor has the apatite configuration.

essential. This fact was further confirmed by x-ray diffraction studies of various calcium halophosphate phosphors. According to the x-ray diffraction patterns of apatite and whitlockite by Prien and Frondel (6), the calcium halophosphate phosphor pattern as shown in Fig. 1 is similar to the apatite structure while tricalcium phosphate is similar to whitlockite. Changing the composition by increasing the manganese or antimony or by varying the ratio of chlorine to fluorine did not alter the structure but only caused a shift in the lattice spacings.

Preparation.—In the preparation of calcium halophosphate phosphors, tricalcium phosphate, C.P. or reagent grade, anhydrous calcium chloride, calcium fluoride, manganese phosphate, and antimony trioxide are ball-milled together. This mixture is then fired in an electric furnace in silica dishes, requiring approximately one hour at 1060°C. for a 300 gram batch. The phosphor can be fired in either air or nitrogen atmosphere with equal results. Oxygen and water vapor, however, produce a discolored phosphor having a poor output.

The final composition of the phosphor is dependent upon the tempera-

ture and time of heating. A portion of the antimony combines with the halides and volatilizes as an antimony halide. As an example, an analysis of a sample of one calcium halophosphate phosphor indicated that 66 per cent of the antimony and 63 per cent of the chlorine were lost during heating. It is thus best to heat the phosphor in a partially stoppered tube so as to prevent excessive volatilization. Heating of the phosphor must be done in well ventilated hoods because of the toxicity of antimony compounds.

Spectral energy distribution.—For the study of the spectral energy distribution of calcium halophosphates, a series of phosphors was prepared having various chlorine to fluorine ratios. Small plaques of these phosphors were irradiated by a quartz Sterilamp and the intensity of fluorescent radiations measured with a Beckman spectrophotometer. It can be seen

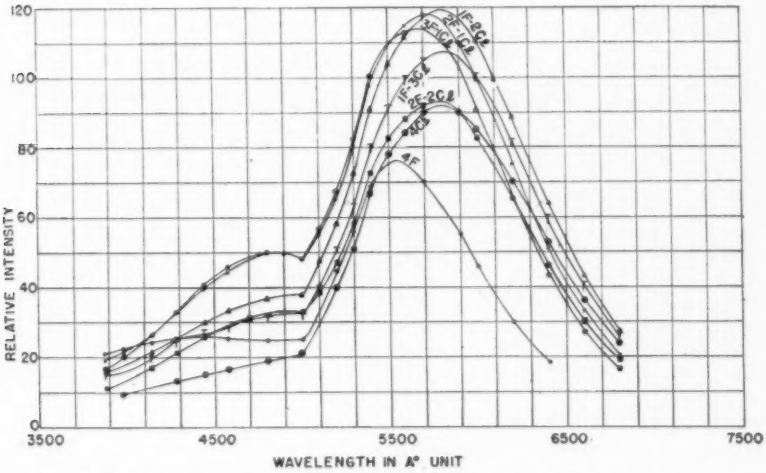

FIG. 2. Spectral energy distribution of calcium halo phosphate with one per cent manganese and with various ratios of chlorine to fluorine.

from Fig. 2 that as the ratio of chlorine to fluorine is increased, the peak of emission of the phosphor is shifted toward the longer wavelength. This peak, however, is also dependent on the amount of manganese in the phosphor. By increasing the manganese content from one per cent, as was used for the phosphors in Fig. 2, to two per cent, the peak of emission was shifted about 50 Å toward the red as shown in Fig. 3. The effect of the variation in the manganese content on the change in the spectral energy distribution is clearly indicated in Fig. 4. The molar ratio of chlorine to fluorine in this phosphor was approximately two to one.

With zero per cent manganese the peak of emission was at about 4800 Å, in the same vicinity as magnesium tungstate. As the percentage of manganese is increased from zero per cent to five per cent, the peak of emission was shifted to about 5850 Å. The original peak, probably due to

antimony, is entirely suppressed and only the emission attributable to manganese is apparent. By varying the ratio of chlorine to fluorine and the amount of manganese in calcium halophosphate phosphor, fluorescent

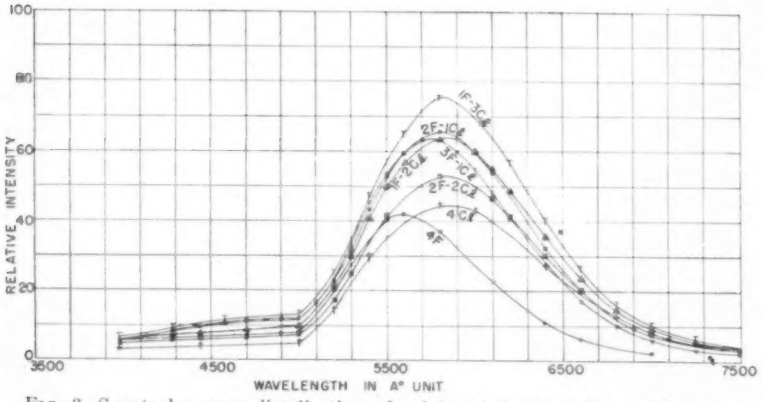

FIG. 3. Spectral energy distribution of calcium halo phosphate with two per cent manganese and with various ratios of chlorine to fluorine.

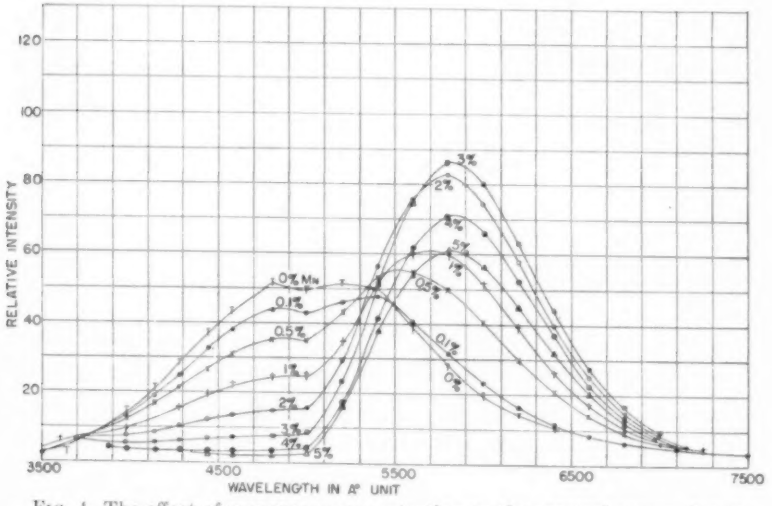

FIG. 4. The effect of manganese concentration on the spectral energy distribution of a calcium halo phosphate having a 1 to 2 ratio of chlorine to fluorine.

lamps can be made to approximate the color temperature of most commercial fluorescent lamps. The amount of antimony in the phosphor does not appreciably affect the fluorescent color (Fig. 5).

Excitation spectra.—Since the calcium halophosphate phosphor was to be used in low pressure mercury discharge tubes, it was of considerable interest to determine whether the excitation spectrum of this phosphor had a maximum at or near 2537 Å, the resonance line of mercury. The method used was the same as that described by Beese (7) except that a grating spectrograph was used instead of a quartz prism instrument. The excitation spectra for various modifications of composition are given in Fig. 6.

There are two distinct peaks of excitation for all the calcium halophosphate phosphors studied. A major one is located at about 2500 Å, and a minor one at about 2200 Å. The intensity of excitation at different wavelengths for each sample was plotted relative to the value of the peak near 2500 Å, taken arbitrarily as 100. Because of the non-uniformity of

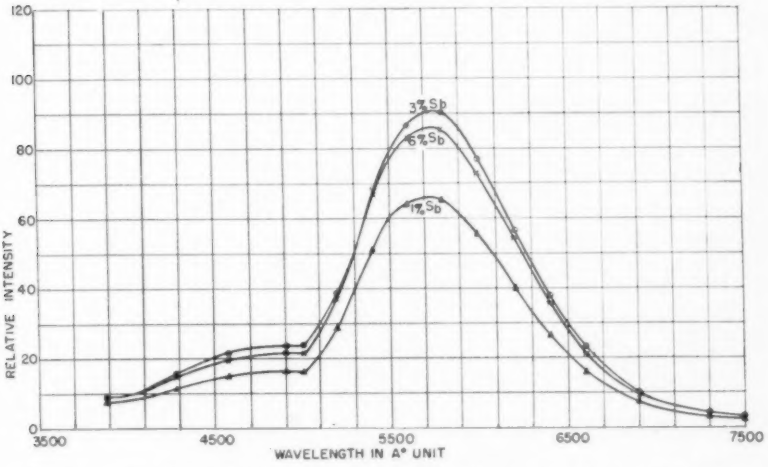

FIG. 5. The effect of the concentration of antimony on the spectral energy distribution of calcium halo phosphate.

the phosphor coating, it is difficult to compare the intensity of excitation of different phosphors with respect to each other.

Inspection of the excitation spectra in Fig. 6 clearly shows that the major peak of excitation with 2 per cent Mn was shifted from 2480 Å by using 100 per cent fluorine as the halide to 2400 Å if 100 per cent chlorine was used instead. If the excitation peak near 2500 Å is the main cause of fluorescence, then the phosphor with larger amounts of fluorine should give a higher fluorescent output, because it utilizes the low pressure mercury resonance line 2537 Å to the best advantage. The effect of manganese seemed to be to enhance the minor excitation peak at 2200 Å. The significance of excitation at 2200 Å is not yet known at the present time.

Effect of impurities.—The tribasic calcium phosphate used in halophosphate manufacture should be of the highest purity. All of the elements

in group two, excluding strontium, have a detrimental effect on the output when present in more than one tenth of a per cent by weight. Strontium can be substituted for calcium up to 20 mol per cent without an appreciable loss of output. Copper, iron, and nickel should be kept well below .01 per cent to give a satisfactory phosphor. Contrary to McKeag and Ranby, bismuth, tin, and lead were not found to be effective substitutes for antimony and were definitely poisonous when used in combination with the activator.

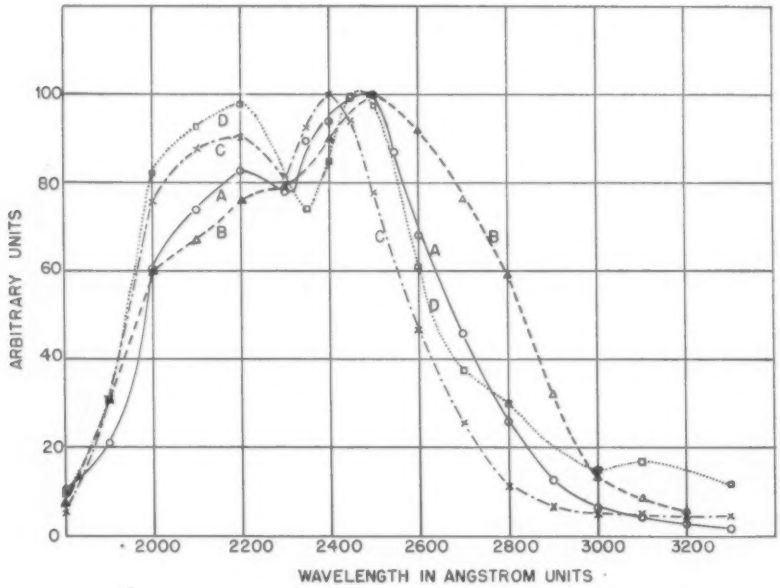

FIG. 6. Excitation of calcium halo phosphate phosphors 5 per cent Sb.
A. $9Ca_3(PO_4)_2 \cdot CaCl_2 \cdot 2CaF_2 \cdot 5\%$ Mn C. $3Ca_3(PO_4)_2 \cdot CaCl_2 \cdot 2\%$ Mn
B. $9Ca_3(PO_4)_2 \cdot CaCl_2 \cdot 2CaF_2 \cdot 0\%$ Mn D. $3Ca_3(PO_4)_2 \cdot CaF_2 \cdot 2\%$ Mn

DISCUSSION

The reaction between calcium chloride or fluoride and calcium phosphate has been shown by x-ray diffraction patterns to give the apatite structure. The addition of antimony and manganese does not alter this structure, but forms a solid solution with the apatite. Antimony can enter readily into the apatite lattice. However, manganese appears to require the presence of antimony before solution can take place. Apatite heated with manganese phosphate is discolored and does not have appreciable fluorescence. The role of antimony, therefore, appears to be twofold, namely, a primary activator and a flux.

The fluorescence of calcium halophosphate activated with antimony has its peak of emission at about 4800 Å. As the percentage of manganese is

increased a new maximum is produced between 5800 Å and 5900 Å (Fig. 4) indicating that the excitation energy is transferred by way of the matrix to the manganese atom. The mechanism of emission apparently is the same as described by Froelich (8) or by Schulman, *et al.* (9). The excitation spectrum indicates that the absorption is in all probability due to the antimony-apatite matrix, as there are no new excitation bands with the addition of manganese. The halides play a small but definite part in determining the peak of excitation.

The mechanism of fluorescent color dependence upon fluorine and chlorine ratios may be similar to that described by Nagy (10). As the amount of distortion in the molecule is increased either by introducing an ion of a low coordination number such as beryllium in zinc beryllium silicate or by resonance as suggested by Anslow (11), the fluorescent color shifts toward the red. According to Beevers *et al.* (12), the structure of apatite would be selective in its choice of ions to occupy the position of fluorine. This would suggest that introducing a larger ion such as chlorine would produce a distortion in the lattice resulting in longer wavelength fluorescence. It would be expected that the bromine and iodine ions because of their still larger size would further distort the apatite lattice. Preliminary results indicate that both bromine and iodine shift the fluorescent spectrum toward the longer wavelengths.

In view of the ease in obtaining fluorescent radiation from calcium halophosphates ranging from blue to orange it was possible to reproduce the color temperatures of the various standard fluorescent lamps. Experimental 40 watt fluorescent lamps made with this phosphor likewise compared very favorably in their light output and maintenance with that of zinc beryllium silicate-magnesium tungstate mixtures used at the present time.

Any discussion of this paper will appear in the discussion section of Volume 95 of the TRANSACTIONS of the Society.

REFERENCES

1. A. H. McKEAG AND P. W. RANBY (To The General Electric Co. Ltd.) British Pat. 578,192, June 19, 1946.
2. A. H. McKEAG AND P. W. RANBY (To The General Electric Co. Ltd.) British Pat. 578,195, June 19, 1946.
3. A. H. McKEAG AND P. W. RANBY (To The General Electric Co. Ltd.) British Pat. 580,363, Sept. 5, 1946.
4. A. H. McKEAG AND P. W. RANBY, *Ind. Chem.*, p. 3, August-September (1947).
5. H. G. JENKINS AND A. H. McKEAG, *J. Gen. Elec. Co. England*, **14**, 232 (1947).
6. E. L. PRIEN AND C. FRONDEL, *J. Urol.*, **57**, 949 (1947).
7. N. C. BEESE, *J. Optical Soc. Am.*, **29**, 278 (1939).
8. H. C. FROELICH, *J. Electrochem. Soc.*, **93**, 101 (1948).
9. J. H. SCHULMAN, L. W. EVANS, R. J. GINTHER, AND K. J. MURATA, *J. Applied Phys.*, **18**, 732 (1947).
10. R. NAGY, "Solid Luminescent Materials," p. 309, John Wiley & Sons, Inc., New York (1948).
11. G. A. ANSLOW, *J. Applied Phys.*, **16**, 41 (1945).
12. C. A. BEEVERS AND D. B. McINTYRE, *Mineralog. Mag.*, **27**, 254 (1946).

ON THE DECAY OF PHOSPHORESCENCE AND THE MECHANISM OF LUMINESCENCE OF ZINC SULFIDE PHOSPHORS[1]

WILLIAM H. BYLER AND GEORGE P. KIRKPATRICK
United States Radium Corporation, New York, New York

ABSTRACT

The decay of phosphorescence of some representative types of zinc sulfide phosphors has been measured. When $I^{-0.5}$ is plotted against t, a series of straight lines is obtained. It is concluded that zinc sulfide phosphors generally obey the second order decay law and that the separate straight lines correspond to emptying of electrons from different trap levels with different rate constants. Samples containing an inhibitor such as nickel may show increasing slopes for the successive decay lines. This is thought to be due to loss of electrons from traps through non-radiative decay.

The results can be explained on the basis of three principal assumptions: (a) A given trap level does not start emptying until the levels above it have emptied to a certain point; (b) The rate of non-radiative decay is constant until late in the decay period; (c) The number of electrons and positive holes eligible for recombination at any instant is the same. A mechanism incorporating these ideas is proposed.

Some significant applications of the theory are discussed. Information about the trapping states is revealed. The theory accounts, at least qualitatively, for many experimental observations.

INTRODUCTION

This paper reports observations on the decay of phosphorescence of some zinc sulfide phosphors and some new points of theory based on the results.

Much of recent thinking on the mechanism of luminescence of the zinc sulfide phosphors has been well summarized by various participants in the Cornell Symposium (1). It is agreed that the delayed emission of radiation is accounted for by the time electrons spend in trapping states. Association of photoconductivity with phosphorescence makes it necessary to conclude that the electrons pass through the conduction band, but there has been a great deal of discussion on the question of the kinetics of the decay, whether it is essentially first or second order. Even though the electrons pass through the conduction band, if they must pass immediately to the positive holes without choice, then the rate of decay is not influenced by the number of holes and the reaction is first order. If, on the other hand, the electrons after being released from traps can be captured by other empty trapping states as well as by positive holes, then the number of holes as well as the number of electrons influences the decay rate and second order kinetics apply.

A strong point favoring the latter mechanism is presented by Urbach,

[1] Manuscript received September 13, 1948. This paper prepared for delivery before the Philadelphia Meeting, May 4 to 7, 1949.

Hemmendinger, and Pearlman (2). They show that the brightness at low levels is proportional to the square of the number of excited states. The form of the decay curve has most often been cited as evidence for a particular mechanism. But this kind of evidence has not been generally accepted as final proof for the reason that it is always possible to fit a second order decay curve by a suitable superposition of first order terms.

Decay data for the sulfide phosphors are usually presented in the form of log-log plots where the curves often approach straight lines over a large part of the decay period and, therefore, suggest second order kinetics. Randall and Wilkins (3) have advanced the view that retrapping is generally a negligible factor and, therefore, that first order kinetics apply. It is recognized (4), however, that at least for the case of a completely exhausted specimen when it is being excited by a low intensity source, retrapping is an important factor. In the absence of decisive evidence to the contrary, it is reasonable to assume that it occurs generally in the zinc sulfide phosphors.

If the decay is considered to be essentially a simple recombination process, which may of course include the trap mechanisms, the following equation applies:

$$I^{-0.5} = I_0^{-0.5} + A^{0.5}t \qquad (1)$$

where I is intensity at time t, I_0 is initial intensity, and A is a constant. Thus, a plot of $I^{-0.5}$ against t should yield a straight line. Nichols and Merritt (5) applied this type plot and found two straight lines which indicated two stages in the decay. One of us (6) later studied the decay of a number of zinc sulfide samples and frequently found three straight lines. We have now extended such treatment of decay data to a wider variety of zinc sulfide specimens and over a wider time range. The straight line plot appears to apply generally. Results of this kind are not compatible with current theories since whenever several processes with different constants are thought to be involved, they are considered as acting simultaneously. Later we shall discuss the results in terms of the band theory of solids.

EXPERIMENTAL METHOD

The decay curves were observed by means of an R. C. A. 931-A electron multiplier tube. One hundred and five volts per stage were applied to the tube from a regulated source. The output of the tube was fed into a Leeds and Northrup galvanometer List No. 2500-F, Type R.

The phosphors were excited by an Air Corps C-5 ultraviolet lamp. The light from the phosphor was then focused on the tube by a concave silvered mirror of 6.5 inch focal length. The response of the tube was tested on the 0.01 and 0.1 shunts of the galvanometer and was found to be linear. The output of the tube was kept within the limits of these shunts by placing neutral density filters between the phosphor and the tube.

The fatigue of the tube was corrected for by repeated observations of a radium excited phosphor.

Since the period of the galvanometer was about 14 seconds a rotating drum phosphoroscope of variable speed was used in observing the decay curves from 0.028 to 30 seconds. No attempt has been made to fit the

various observed sections of the curves together, since the duration and levels of excitation varied widely. (The initial brightness of the phosphors ranged from 30 to 150 microlamberts.)

RESULTS

In Fig. 1, 2, and 3 are shown decay data for three different types of zinc sulfide phosphors on both log-log and reciprocal square root plots. The

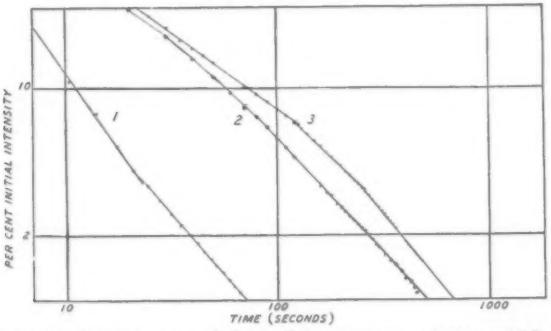

FIG. 1. Log-log decay curves of three different types of zinc sulfide phosphors: 1. ZnS·Ag; 2. ZnS(88)CdS(12)·Cu; 3. ZnS·Cu. The decay curves of different specimens of a given type may vary widely depending on method of preparation and proportions of constituents.

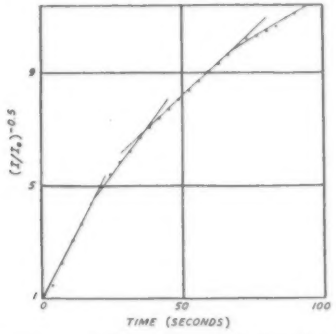

FIG. 2. Reciprocal square root decay curve of phosphor 1 of Fig. 1.

repeated appearance of series of straight lines on the latter type plot is considered as evidence that in the time range under consideration in this paper, the decay of the zinc sulfide phosphors generally follows the second order decay law.

It is instructive to compare the two types of plots. The equations for the second order law are as follows:

$$I = -dn/dt = An^2 \tag{2}$$

$$I = An_0^2/(n_0 At + 1)^2 \tag{3}$$

where I is intensity at time t, n is the number of excited states at time t, n_0 is the initial number, and A is the rate constant. Therefore at large t,

$$\log I/\log t \sim (\log \frac{1}{A}/\log t) - 2 \tag{4}$$

As the decay proceeds, the slope of the log-log plot approaches -2. But the plot should gradually curve downward. If the data plot as a perfectly straight line over a long range or if there is a sharp break downward or especially if there is an upward break, it is evident that a straightforward application of the second order law in the usual manner is not

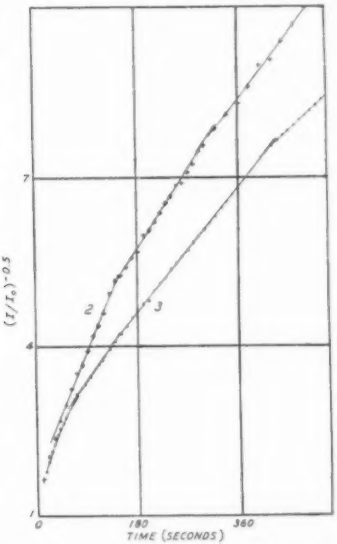

FIG. 3. Reciprocal square root decay curves of phosphors 2 and 3 of Fig. 1.

justified. It is observed in Fig. 1, 2, and 3 that breaks in the log-log curves sometimes coincide with breaks in the reciprocal square root plots.

Equation (3) can be put in the following form:

$$\begin{aligned} I^{-0.5} &= I_0^{-0.5}(1 + An_0t) \\ &= I_0^{-0.5} + (An_0^{\frac{3}{2}})^{-0.5} An_0t \\ &= I_0^{-0.5} + A^{0.5}t \end{aligned} \tag{5}$$

$$(I^{-0.5} - I_0^{-0.5})/t = A^{0.5} \tag{1}$$

Therefore, when the reciprocal square root plot yields a series of straight lines, the obvious conclusion is that different specific decay constants are operating over different portions of the decay period. The different constants are evidently associated with different trap levels. It is clear why the log-log curves do not have the regular form required by the second order equations with a single constant.

The rate constants must decrease for successively lower trap levels if the trap release constants are the only variable factors in the overall rate constants. The trap release constants decrease with increasing trap depth because $A_i = Se^{-E_i/kt}$ where S is a constant and E_i is trap depth.

Putting equation (3) in the following form,

$$An^2 = An_0^2/(n_0At + 1)^2$$
$$t = [(I_0/I)^{0.5} - 1]/n_0A, \tag{6}$$

the time required for decay to any fraction of the initial intensity is greater for smaller A which means smaller slope, so that the log-log plot tends to

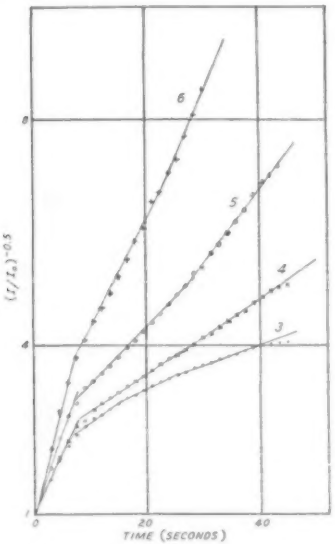

FIG. 4

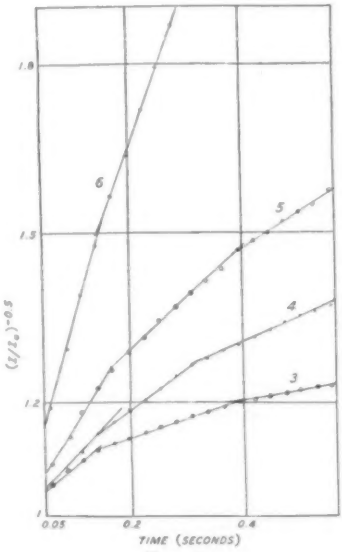

FIG. 5

FIG. 4. Reciprocal square root decay curves of ZnS·Cu phosphors containing different amounts of nickel: 3. No nickel; 4. 0.5×10^{-6}g. Ni/g.; 5. 10^{-6}g. Ni/g.; 6. 2×10^{-6} g. Ni/g.

FIG. 5. Reciprocal square root decay curves of ZnS·Cu phosphors containing different amounts of nickel. The same phosphors as in Fig. 4.

break upward when a smaller A becomes the determining rate constant. This occurs in Fig. 1. We are dealing here with the portion of the log-log plot before the theoretical slope of -2 has been reached.

From the above considerations alone, the successive legs of the reciprocal plot should be expected always to have decreasing slope, but Fig. 4 and 5 show that addition of nickel may cause the slope to break upward. We conclude that this is due to loss of electrons from traps through non-radiative decay. It seems significant that the plot remains a succession of straight lines in the face of such non-radiative loss. We find that this

is what would happen if the loss were constant in amount during the time covered by these data. This loss also accounts for the sharp breaks downward in the log-log curves as well as curves with slope greater than 2 which are sometimes observed. In other cases when the log-log curve remains essentially straight in the face of a change in A shown by the reciprocal plot, it is concluded that the tendency toward an upward break required by smaller A is balanced by the greater proportional non-radiative loss. It can be seen, then, that study of both types of plots can sometimes yield more information than study of either alone.

THEORETICAL

A mechanism compatible with the above results must include three principal features: (a) A given trap level does not start emptying until the trap levels above it have emptied to a certain point; (b) The rate of non-radiative decay is constant until late in the decay period; (c) The number

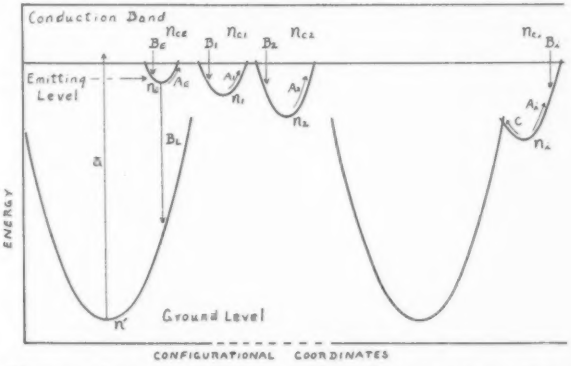

FIG. 6. Diagram of proposed luminescence mechanism for the sulfide phosphors. The broken line indicates spatial separation of the different states.

of electrons and positive holes eligible for recombination at any instant is the same.

The theory can best be discussed with reference to the diagram of Fig. 6 which is based on the band theory of solids as applied to luminescence by Johnson (7) and the scheme for non-radiative decay advanced by Seitz (8). A diagram of this kind is, of course, a highly idealized picture of the mechanism, but helps in both the development and presentation of the essential ideas. The question of the existence of "impurity" levels above the full band from which electrons may be excited and to which they fall is not considered here, although such levels could be included without affecting the argument. We assume that the depth of a trap increases with its distance from the absorbing and emitting region. A "center" may be considered as including the whole system of absorbing, emitting, and trapping levels.

Absorption of an exciting quantum raises an electron from the ground level to the conduction band. The rate at which this occurs is $dn'/dt =$

$aI_e n'$, where n' is the number of electrons in excitable levels at time t, I_e is exciting intensity, and a is a constant.

The number of electrons in the conduction band at time t is represented by n_c. The electron concentration in different regions of the conduction band may vary. These electrons can go to an emitting level or to any of the traps with the corresponding capture cross section B_E, B_1, etc.

The A's are the respective probability constants for thermal release of electrons from the traps and the emitting level into the conduction band.

The energy curves of the ground state and the lowest trapping state cross giving rise to a probability of non-radiative release of electrons from this trap, represented by C.

The number of electrons in the various levels is represented by n_1, etc., and n_{1E}, etc. represent the number of empty states of the various kinds at time t. We assume that the various potential empty states are non-functioning whenever there is no positive hole in the immediate vicinity.

The probability of radiative transition from the emitting level is B_L.

The rates of change of numbers of electrons in the various states are as follows:

$$\begin{aligned}
dn_E/dt &= B_E n_{cE} n_{EE} - A_E n_E - B_L n_E \\
dn_c/dt &= A_E n_E - B_E n_{cE} n_{EE} + A_1 n_1 \\
&\quad - B_1 n_{c1} n_{1E} + A_2 n_2 - B_2 n_{c2} n_{2E} \\
&\quad + A_i n_i - B_i n_{ci} n_{iE} \\
dn_1/dt &= B_1 n_{c1} n_{1E} - A_1 n_1 \\
dn_2/dt &= B_2 n_{c2} n_{2E} - A_2 n_2 \\
dn_i/dt &= B_i n_{ci} n_{iE} - A_i n_i - C n_i
\end{aligned}$$

Let us assume that excitation is prolonged until equilibrium is reached, i.e., the concentration of electrons in the various states is constant. Due to the difference in distance from the point where electrons are emptied into the conduction band by excitation, the concentration of electrons above the different traps is different, i.e., $n_{c1} > n_{c2} > n_{ci}$. It is, of course, necessary to assume that electrons in the conduction band may pass freely from center to center.

Now when excitation stops, since B_L is large, n_{cE} quickly decreases. The electrons above trap 1 move in the direction of the emitting level. Since n_{c1} is now decreased, $A_1 n_1$ becomes greater than $B_1 n_{c1} n_{1E}$ and dn_1/dt is a negative quantity signifying that trap 1 is emptying. But since n_{c1} is greater than n_{c2}, electrons cannot move from trap 2 toward the emitting level, and so on. Therefore, the lower trap maintains a constant population until trap 1 empties to a certain point. The overall decay constant is related to the other constants as follows: $A \propto (A_1, \text{etc.}/B_1, \text{etc.})\,(B_E/A_E)$-$B_L$. Since B_E, A_E, and B_L are constants independent of different trap levels, the trap constants, A_1, etc. and B_1, etc. determine the overall constant, and since during this early period the lower traps are dormant, A_1 and B_1 are the only trap constants influencing the decay rate.

When trap 1 has decayed to the point where $n_{c2} = n_{c1}$, electrons can flow from trap 2 to the emitting level. If trap 1 were operating independently after this time, n_{c1} would decrease faster than it now can. The supply of electrons from trap 2 maintains the equality of n_{c1} and n_{c2}. Thus trap 1 now empties at a slower rate and, in fact, the trap constants of

trap 2 assume control which accounts for the break in the reciprocal square root plot. The electrons remaining in trap 1 have the effect of adding to the number in trap 2.

There may be any number of trap levels depending on the phosphor, but finally we consider the effect of a low trap level from which non-radiative transitions can originate. (Such a non-radiative mechanism in a different context has been suggested by Williams and Eyring (9).) In order for n_i to remain constant, the following must hold:

$$B_i n_{ci} n_{iE} = Cn_i + A_i n_i$$

As long as the upper traps are emptying electrons so that n_{ci} remains high enough to maintain this equality, the non-radiative loss is at a constant rate, Cn_i. In the cases of the other traps, the filling and emptying during decay of a higher trap had no influence on decay rate. But here Cn_i fewer electrons per unit time are fed back than leave the conduction band. Therefore, until n_{ci} decreases to the point where $B_i n_{ci} n_{iE} < Cn_i + A_i n_i$, this effect is the same as subtracting a constant intensity. When n_{ci} does reach this point, the reciprocal square root plot should digress from a straight line unless this level is completely non-radiating, i.e., $A_i = 0$. This follows from the fact that a first order effect would be subtracted from a second order one. For a given phosphor at constant temperature, C is constant. But C my be increased by adding an inhibitor such as nickel.

The third point listed at the beginning of this section remains to be discussed. The step-wise decay scheme implies that, at most, only those electrons in the emptying trap levels are influencing the decay rate during that part of the decay period. This suggests that early in the decay period many more positive holes than electrons are influencing the rate. Such an imbalance carried to extremes might modify the decay law. But the present treatment suggests an equal number of electrons and positive holes active at any instant. We suggest the following hypothesis to account for this.

Positive holes, like electrons, are effectively free only when electrons are in the conduction band. Thus, when an electron is in a trapping state, there must be a positive hole in the vicinity and this positive hole is not effective as an electron receptor. When the electron is raised from the trap into the conduction band, the corresponding hole is then also free to move. The pair, not necessarily the original individuals, may reunite at the site of another trapping state or at the site of an emitting state. If at the former, complete recombination is, of course, forbidden; if at the latter, recombination may occur.

In the next section some applications of the theory will be discussed, largely in a qualitative way.

SOME APPLICATIONS

Trap populations.—Trap level populations can be found by calculating light sums under the various legs of decay if correction is made for non-radiative loss. According to the above theory, the correction can be found from fluorescence quantum efficiency measurements, since the rate of non-radiative loss at a given temperature and intensity is the same during excitation as it is during the early legs of decay.

To get the population for a given level, the straight line corresponding to its decay constant is mathematically extended to infinity since the level would continue to empty at the same specific rate with which it started if there were no lower traps. From the light sum thus calculated is subtracted the sum representing the contribution by higher traps during this period. Putting equation (1) in the following form,

$$I = 1/(A^{0.5}t + I_0^{-0.5})^2$$

$$\int_{t_1}^{t_2} I\,dt = [-1/A^{0.5}(A^{0.5}t + I_0^{-0.5}]_{t_1}^{t_2},$$

$A^{0.5}$ is the slope of the line and $I_0^{-0.5}$ is the intercept on the zero time ordinate.

Applying this method to a copper-activated zinc sulfide phosphor and assuming 90 per cent quantum efficiency, the following results were obtained:

	Trap 1	*Trap 2*	*Trap 3*	*Trap 4*
Light sum from beginning to infinity	67	103.6	125.5	189.5
Remaining at next break	53.5	87.6	107.6	163.5
Trap population		50.1	37.9	81.9

The population of the level represented by the first line cannot be obtained from these data because it is known that other levels lie above it.

The striking point about these results is that a given trap level starts emptying when there still remain more electrons in higher traps than the total number in the trap in question. Of course, the magnitude of the assumed quantum efficiency has a large influence on the calculated relative populations, but we find the above phenomenon holding in many cases in the face of any reasonable quantum efficiency. It is, therefore, necessary to conclude that the capture cross sections, B, are widely different for the different trap levels.

This method may be expected to give more accurate results than glow curve measurements since, in that case, the amount of non-radiative loss is varying with temperature. Also in that case, measurement of the points of separation between levels is not as precise, although high accuracy is not claimed for the present method.

Trap depths.—On account of the differences in capture cross sections of the trap levels, we cannot calculate differences in trap depths, but it is worthwhile to examine the relationships involved for the sake of clarifying the proposed mechanism.

According to equation (1), the slope of the straight line represents the square root of the specific rate constant so we can measure this constant, A_m.

$$A_{m1} = KA_1 B_E B_L / B_1 A_E$$

$$A_{m2} = KA_2 B_E B_L / B_2 A_E$$

$$A_1/A_2 = (A_{m1}/A_{m2})(B_1/B_2)$$

$$A_1, \text{ etc.} = S\, e^{-E_1, \text{ etc.}/kt}$$

$$E_2 - E_1 = kT\, ln[(A_{m1}/A_{m2})(B_1/B_2)]$$

Now if the capture cross sections, B, were equal, trap level separations could be calculated from the measured line slopes, after correction for non-radiative loss.

The significant point here is that if B_1 is greater than B_2, the actual level separation is greater than would be indicated by the measured slopes. Since the actual separation, $E_2 - E_1$, is a fixed quantity, any ratio B_1/B_2 greater than unity will require a reduced ratio A_{m1}/A_{m2} which is the measure of effective separation. This is in line with the above observation that it is possible for a lower trap level to start emptying when a higher level still contains more electrons.

Fluorescence intensity as a function of temperature, exciting intensity, and inhibitor (poison, killer) content.—These variables will be considered together because they are interrelated as shown by Nail, Pearlman, and Urbach (10). Klasens and associates (11) and Kröger (12) have developed a hole migration theory which they believe accounts for many experimental results.

Urbach, Urbach, and Schwartz (13) have suggested that much of the data relating fluorescence intensity to exciting intensity can be accounted for by assuming that the radiative process is second order while the non-radiative process is first order. They did not propose a mechanism. In our scheme, the first order non-radiative process is based on thermal transfer of electrons from a trapping level to the ground level as designated by C in Fig. 6.

$$\begin{aligned} dn_E/dt &= B_E n_{cE} n_{EE} - A_E n_E - B_L n_E = 0 \\ I = B_L n_E &= B_E n_{cE} n_{EE} - A_E n_E \\ dn_c/dt &= an' I_e + A_E n_E - B_E n_{cE} n_{EE} \\ &\quad + A_i n_i - B_i n_{ci} n_{iE} = 0 \\ B_E n_{cE} n_{EE} &= an' I_e + A_E n_E + A_i n_i - B_i n_{ci} n_{ie} \end{aligned} \tag{7}$$

Substitute in (7): $I = an' I_e - (B_i n_{ci} n_{iE} - A_i n_i)$

$$\begin{aligned} dn_i/dt &= (B_i n_{ci} n_{iE} - A_i n_i) - C n_i = 0 \\ I &= an' I_e - C n_i \end{aligned} \tag{8}$$

This is similar to Urbach's equation except that it includes the number of electrons in excitable states, n', and it substitutes n_i, the number of electrons in the leak trap level, for his n, the number of excited states. From equation (8), as long as the exciting intensity is high enough to maintain n_i constant, the non-radiative loss is constant whereas according to Urbach's equation the non-radiative loss changes continuously with exciting intensity. Our scheme requires that as I_e is decreased from a certain high level down to a certain lower level, a constant quantity is subtracted from the straight line log-log plot (13); below that level a decreasing quantity is subtracted. This results in a gradual curvature downward until the loss represents a substantial proportion of the total when the curve breaks sharply. A gradual decrease of the loss then tends to straighten the line again corresponding to the shape which is actually observed. It is clera then why samples measured at high temperature, which increases C, or samples containing an inhibitor, which increases the loss through increase of C or some other means, show large downward curvature. There is no reason to expect a limiting slope of 2.

The factor n' in equation (8) is variable and may come into play noticeably at the extremes of the range of exciting intensity. At very high intensities the electrons spend shorter average time in the ground state so that n' is lower and tendency toward saturation may be observed. At low intensities the traps are not completely filled and n' is higher. This effect would tend to cause the plot to curve back upward as one of Urbach's curves shows.

Klasens' (14) curves showing fluorescence intensity as a function of temperature for phosphors containing varied nickel, as well as Garlick's (15) and Nail, Pearlman, and Urbach's (16) curves showing fluorescence intensity as a function of temperature for varied exciting intensity, can be explained in terms of the mechanism we propose. The extremely low efficiency at high temperature cannot be due to an effect of temperature on C alone. But A_E also increases with temperature and at a greater rate than does A_i. This differential increases the relative probability of capture by the leak level and may well account for a decrease of efficiency to zero.

As temperature is increased, many zinc sulfide phosphors change color toward longer wavelengths. This is compatible with our picture if we assume different effective capture cross sections for the different emission bands. The effective capture cross section is proportional to B_E/A_E. Therefore, the nearer the emitting level is to the conduction band, the smaller is the effective capture probability for a given B. A given increase of temperature would decrease the effective capture probability of a shallow emitting level faster than that of a deeper level.

While the proposed mechanism appears to account at least qualitatively for many experimental observations, it is obvious that much remains to be done before it can be considered to be firmly established.

Any discussion of this paper will appear in the discussion section of Volume 95 of the TRANSACTIONS of the Society.

REFERENCES

1. G. R. FONDA AND F. SEITZ, Editors, "Cornell Symposium," John Wiley & Sons, Inc., New York (1948).
2. *Ibid.*, p. 294.
3. J. T. RANDALL AND M. H. F. WILKINS, *Proc. Roy. Soc. London*, A, **184**, 390 (1945).
4. G. F. J. GARLICK, ref. 1, p. 97; F. URBACH, ref. 1, p. 128.
5. E. L. NICHOLS AND E. MERRITT, "Studies in Luminescence," Carnegie Inst. of Wash. (1912).
6. W. H. BYLER, *J. Am. Chem. Soc.*, **60**, 632 (1938).
7. R. P. JOHNSON, *J. Optical Soc. Am.*, **29**, 387 (1939).
8. F. SEITZ, "The Modern Theory of Solids," p. 452, McGraw-Hill Book Co., Inc., New York (1940)
9. F. E. WILLIAMS AND H. EYRING, *J. Chem. Phys.*, **15**, 289 (1947).
10. N. R. NAIL, D. PEARLMAN, AND F. URBACH, ref. 1, p. 190.
11. H. A. KLASENS, *Nature*, **158**, 483 (1946); H. A. KLASENS, W. RAMSDEN, AND C. QUANTIE, *J. Optical Soc. Am.*, **38**, 60 (1948); M. E. WISE AND H. A. KLASENS, *J. Optical Soc. Am.*, **38**, 226 (1948).
12. F. A. KRÖGER, "Some Aspects of the Luminescence of Solids," p. 223 ff., Elsevier, N. Y. (1948)
13. F. URBACH, A. URBACH, AND M. SCHWARTZ, *J. Optical Soc. Am.*, **37**, 122 (1947).
14. H. A. KLASENS, ref. 1, p. 200.
15. G. F. J. GARLICK, ref. 1, p. 113.
16. N. R. NAIL, D. PEARLMAN, AND F. URBACH, ref. 1, p. 199.